

Hunting Tools Beyond the Driplines

Performing large-scale nuclear physics experiments

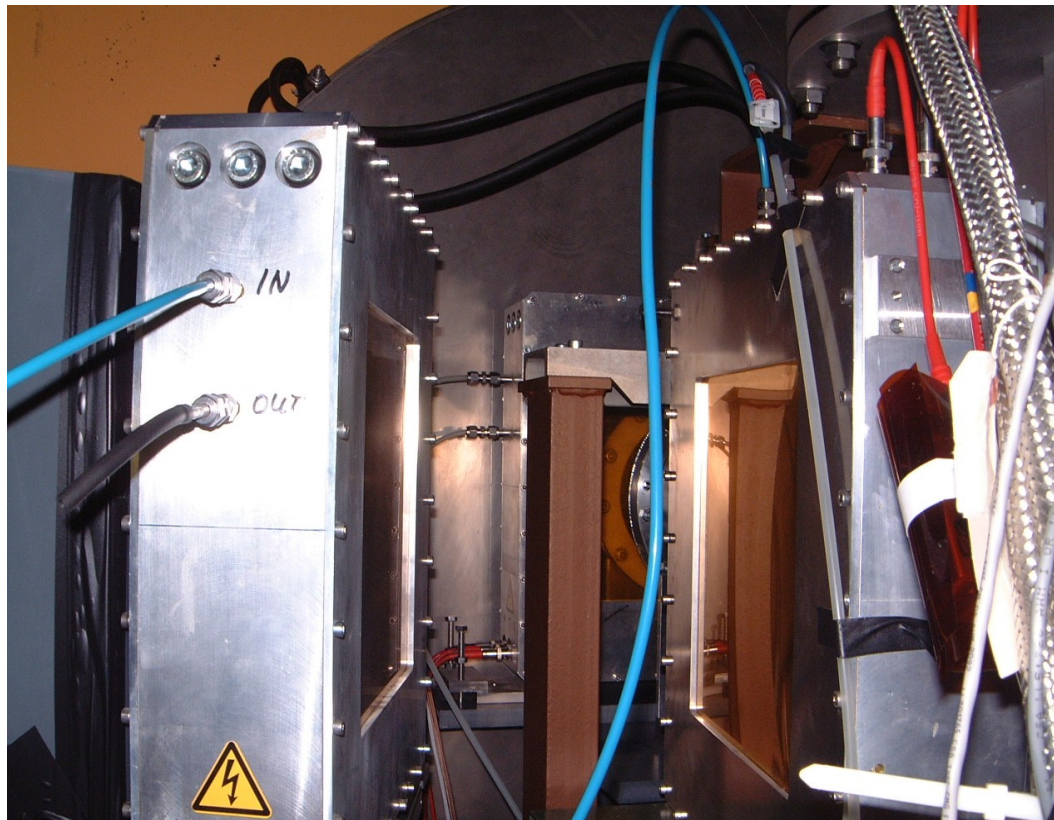
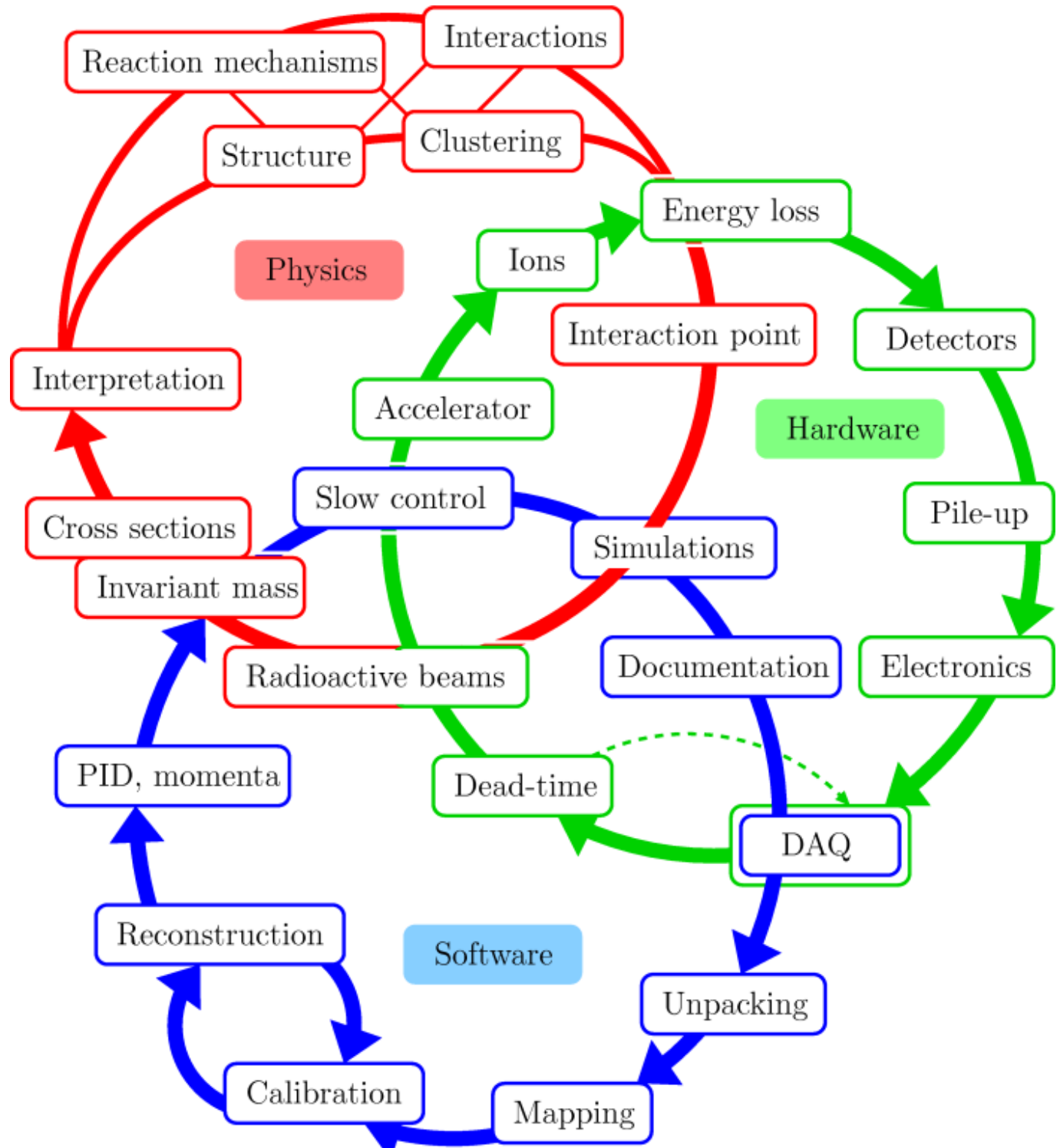
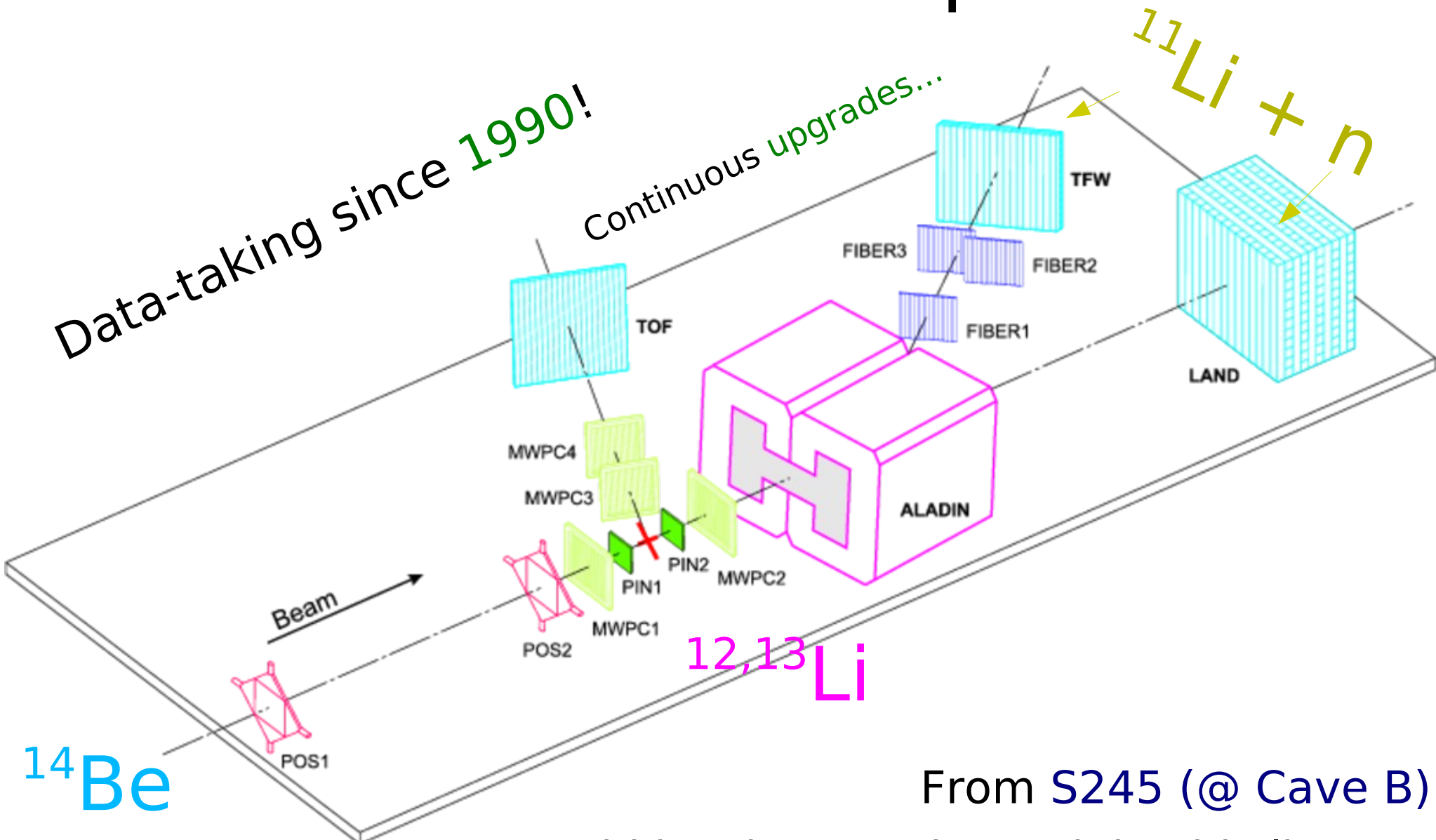


Table of Contents.



ALADiN-LAND setup → R³B



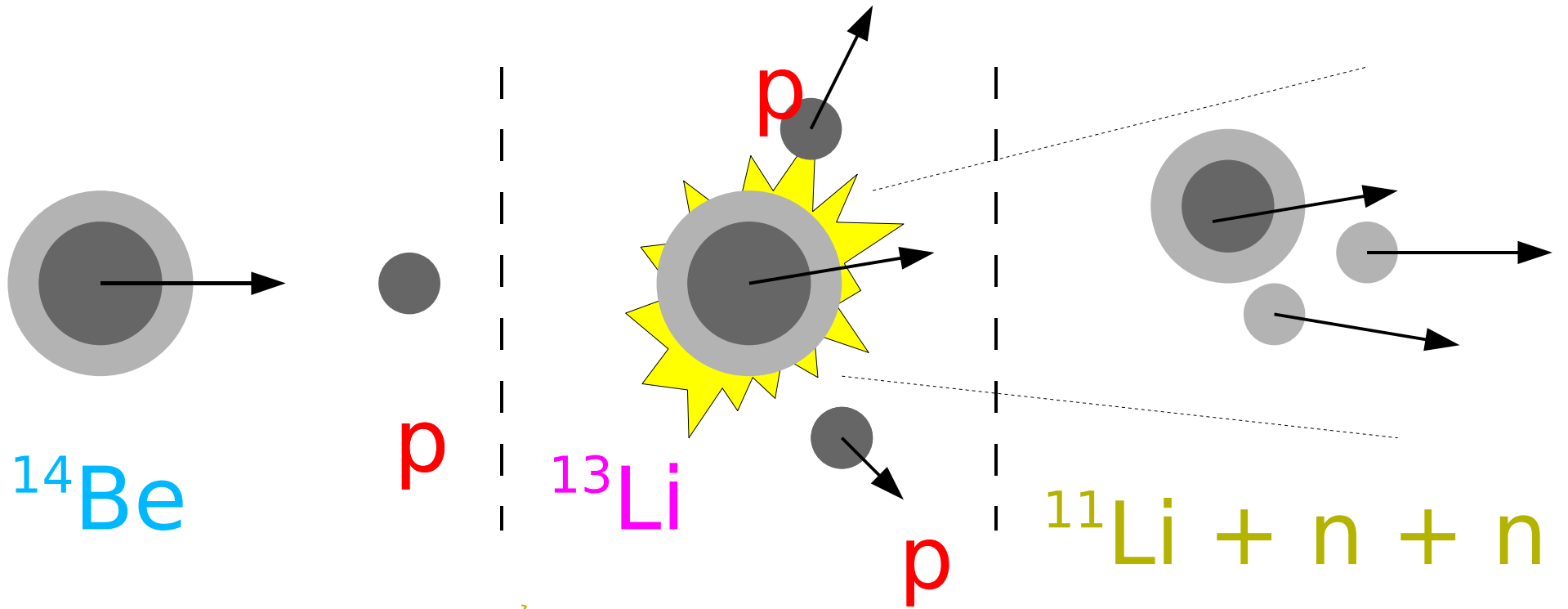
From S245 (@ Cave B):

Lithium isotopes beyond the drip line

Yu. Aksyutina, H.T. Johansson, et. al.

Physics Letters B, Vol 666 (2008) pp. 430-434

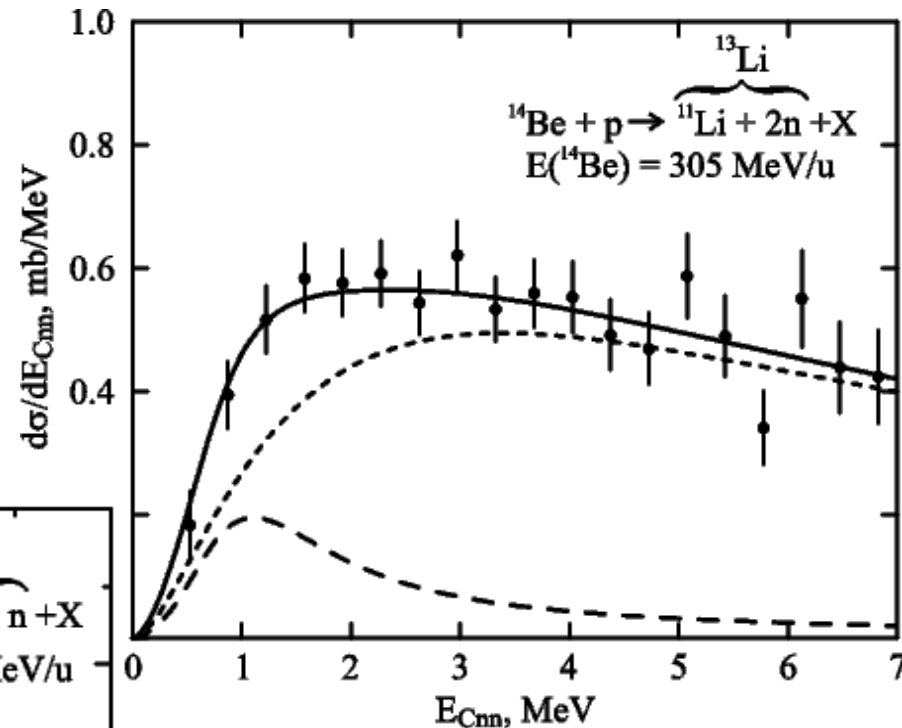
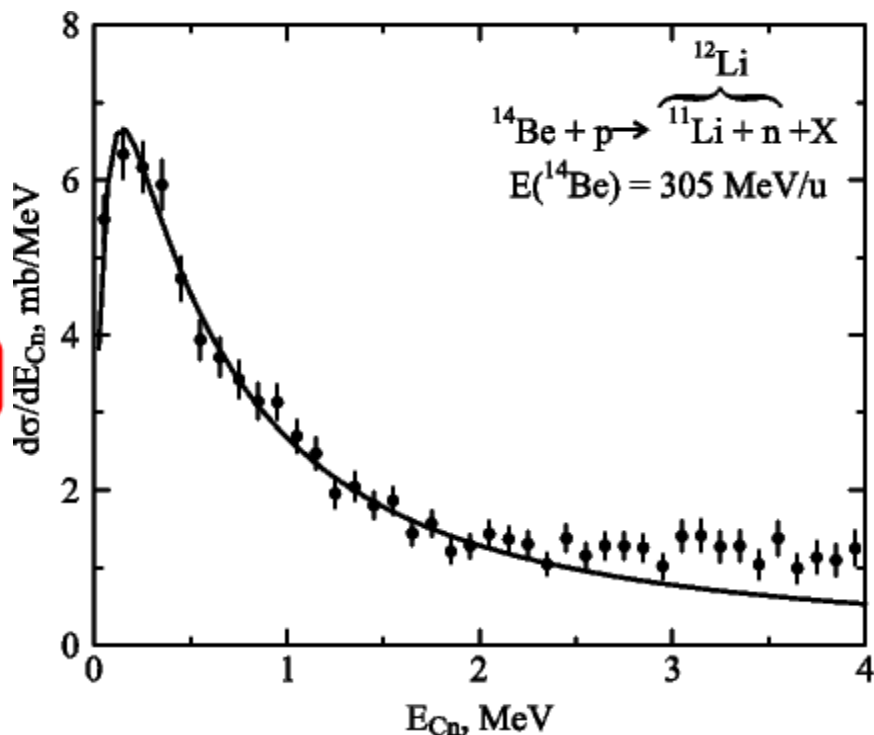
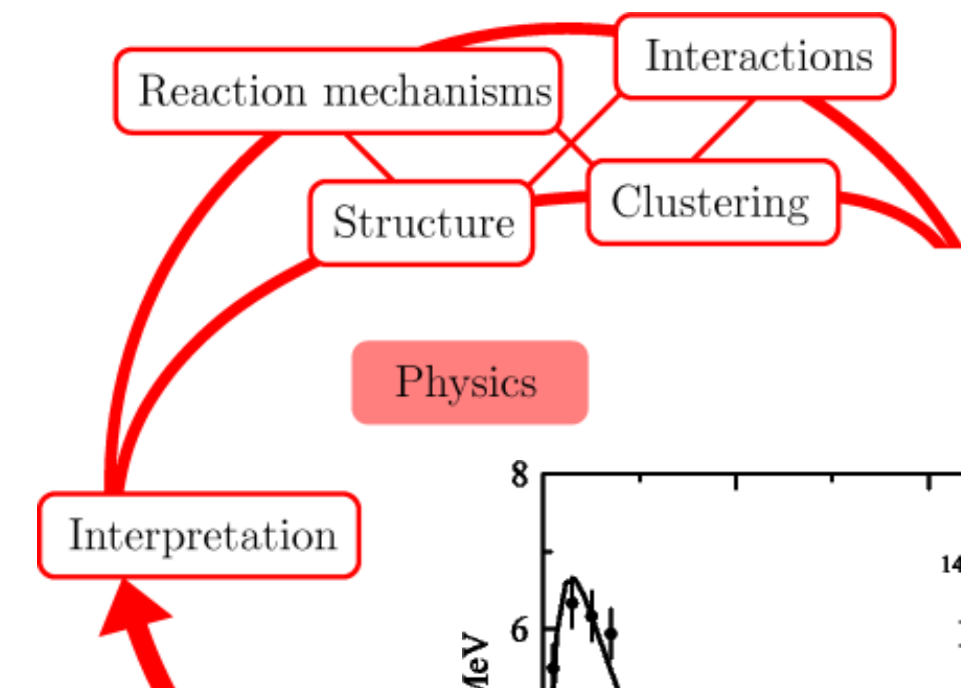
Unbound systems via invariant mass



$$\mathbf{p}_{^{13}\text{Li}} = \mathbf{p}_{^{11}\text{Li}} + \mathbf{p}_n + \mathbf{p}_n$$

$$-\mathbf{p}_{^{13}\text{Li}}^2 = m_{^{13}\text{Li}}^2$$

The unbound $^{12,13}\text{Li}$ observed for the first time



Invariant mass
spectra

Ions

Accelerator

GSI (Darmstadt, Germany)

ACCELERATOR FACILITIES
AND EXPERIMENTAL AREAS

PENNING,
CHORDIS &
MEVVA
ION SOURCES

ECR ION SOURCE

HLI



UNILAC

LOW ENERGY
EXPERIMENTAL
AREA

RADIOTHERAPY

CAVE A

TARGET
AREA

0 50 m



SIS

FRS

PLASMA
PHYSICS

PION PROD.-
TARGET

HADES

CAVE C

CAVE B

Gesellschaft für
Schwerionenforschung mbH

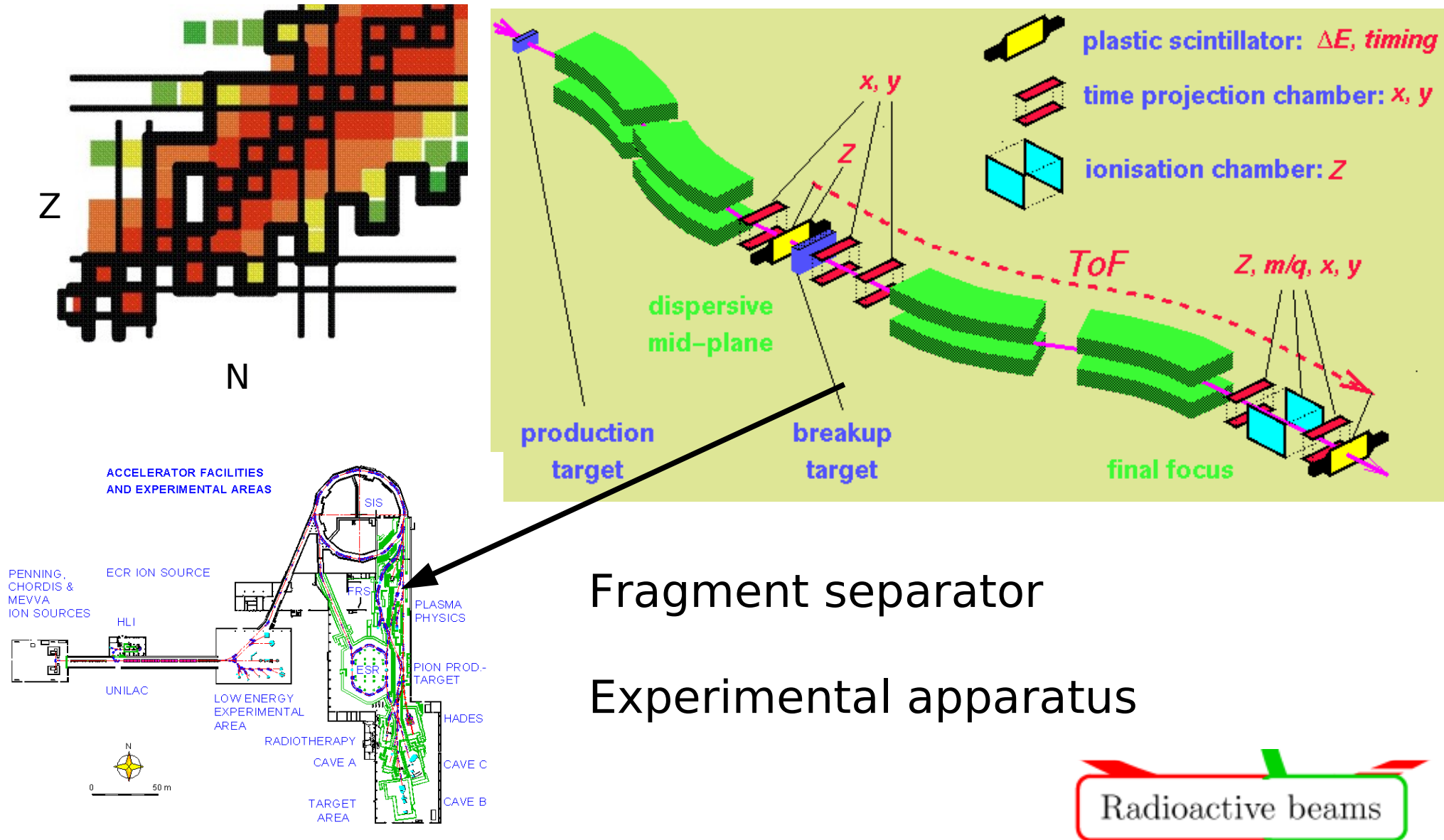
Fragment separator (FRS)

ALADiN-LAND setup

2005-

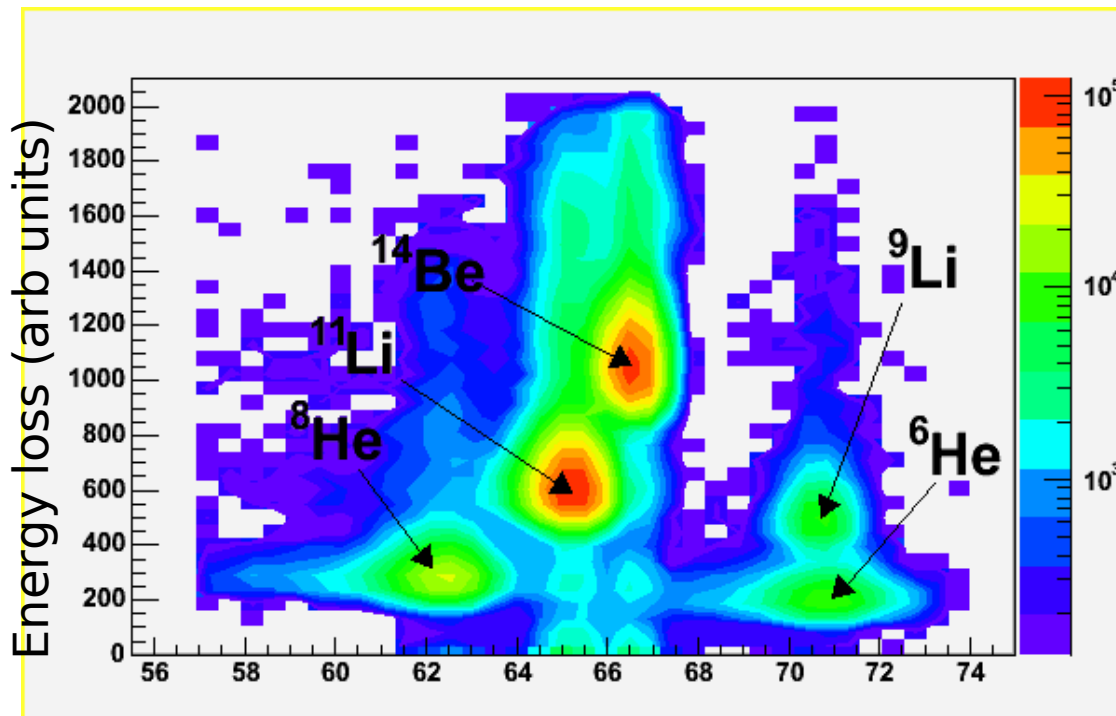
1990-2004

Exotic isotope production & selection



PID, momenta

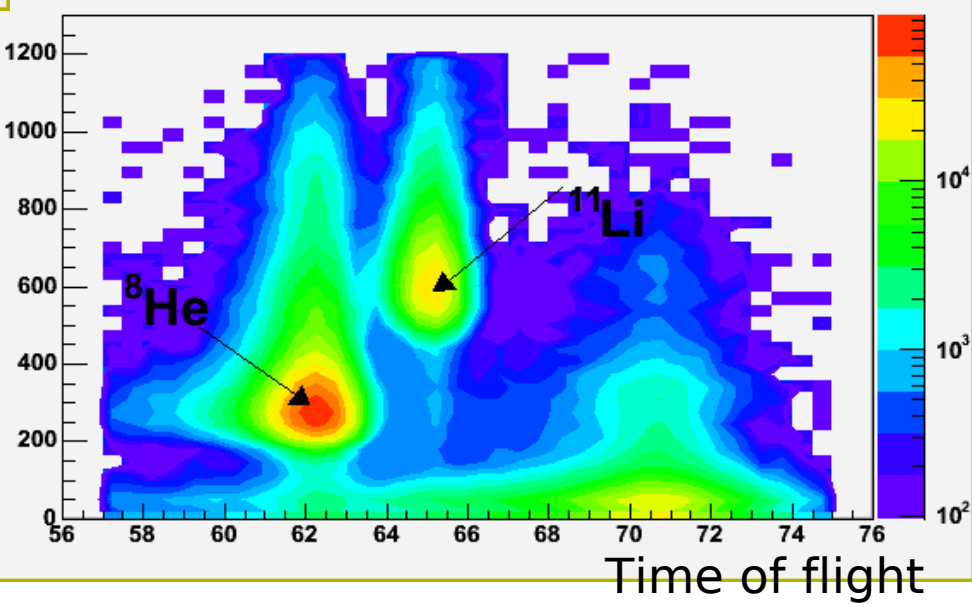
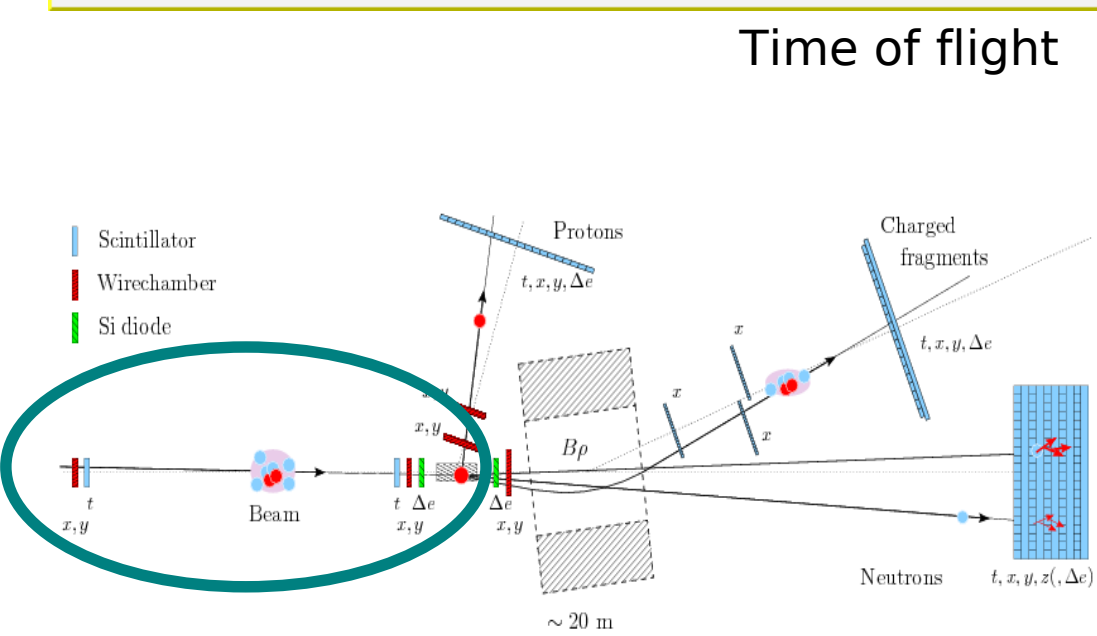
Incoming beam identification



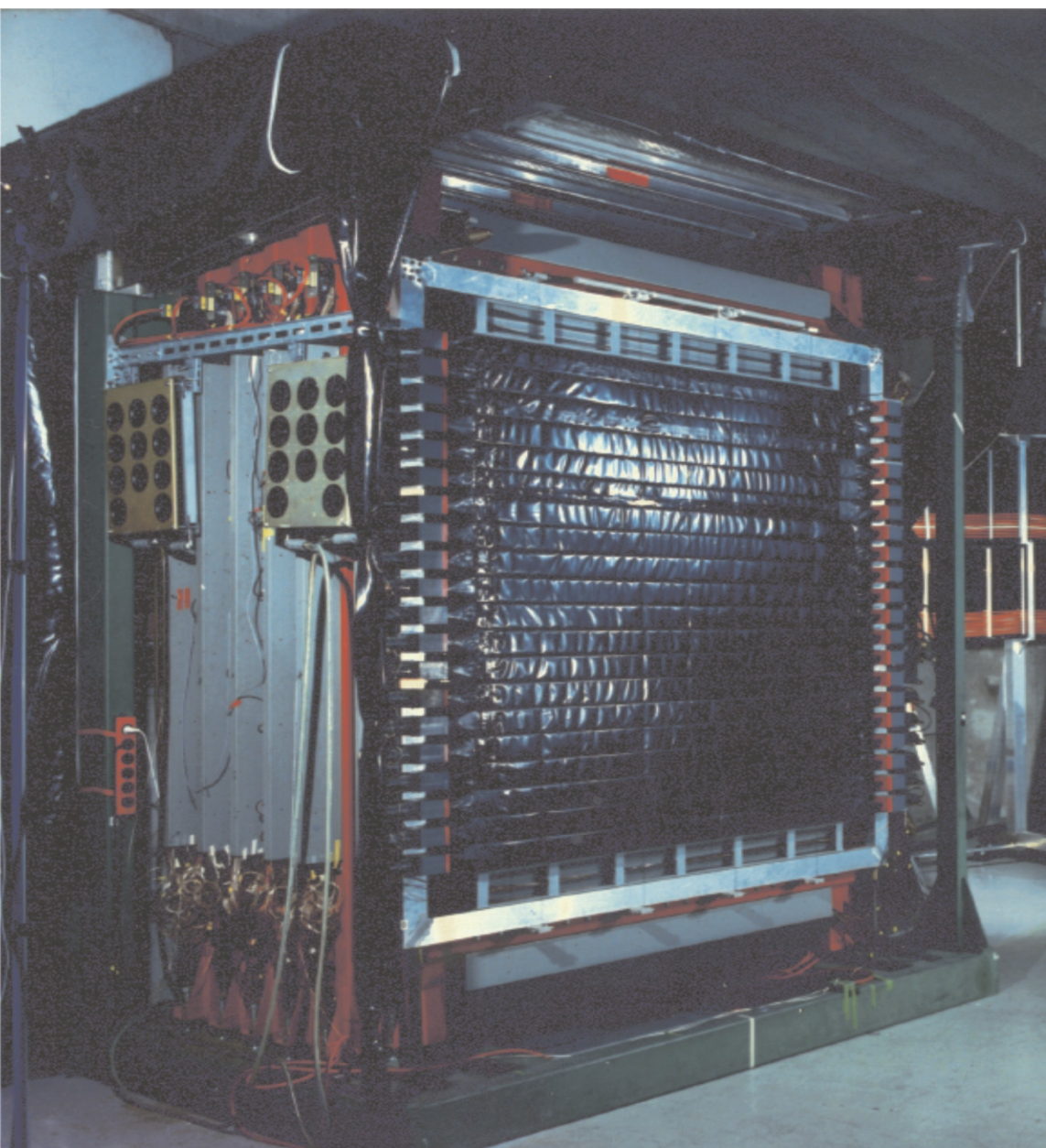
Ion charge (Z) from energy loss.

Ion mass (A), from A/Z , from velocity (time-of-flight).

Ions surviving the fragment separator selection have velocity depending on their A/Z .



LAND - Large area neutron detector



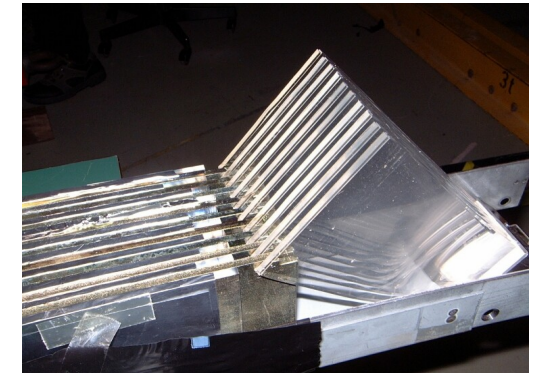
Volume: $2 \times 2 \times 1 \text{ m}^3$

Detectors

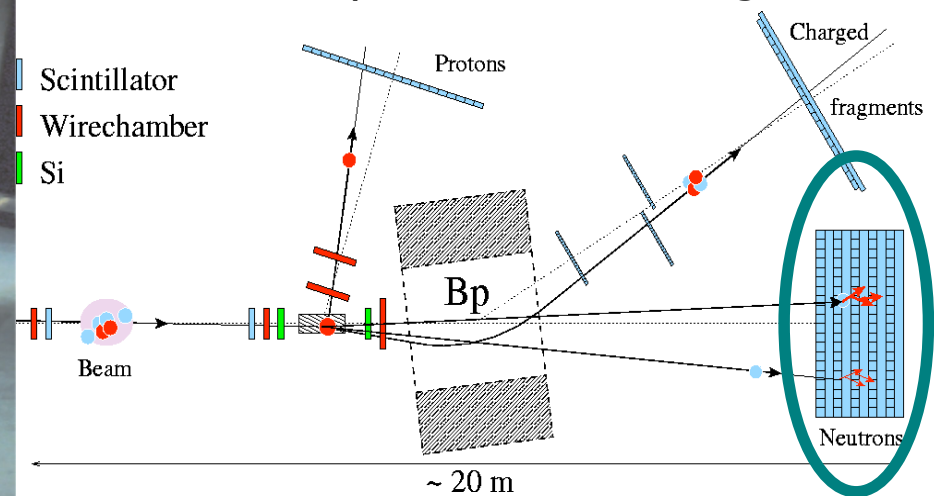
10x20 paddles

sandwiched: iron converter and
scintillator

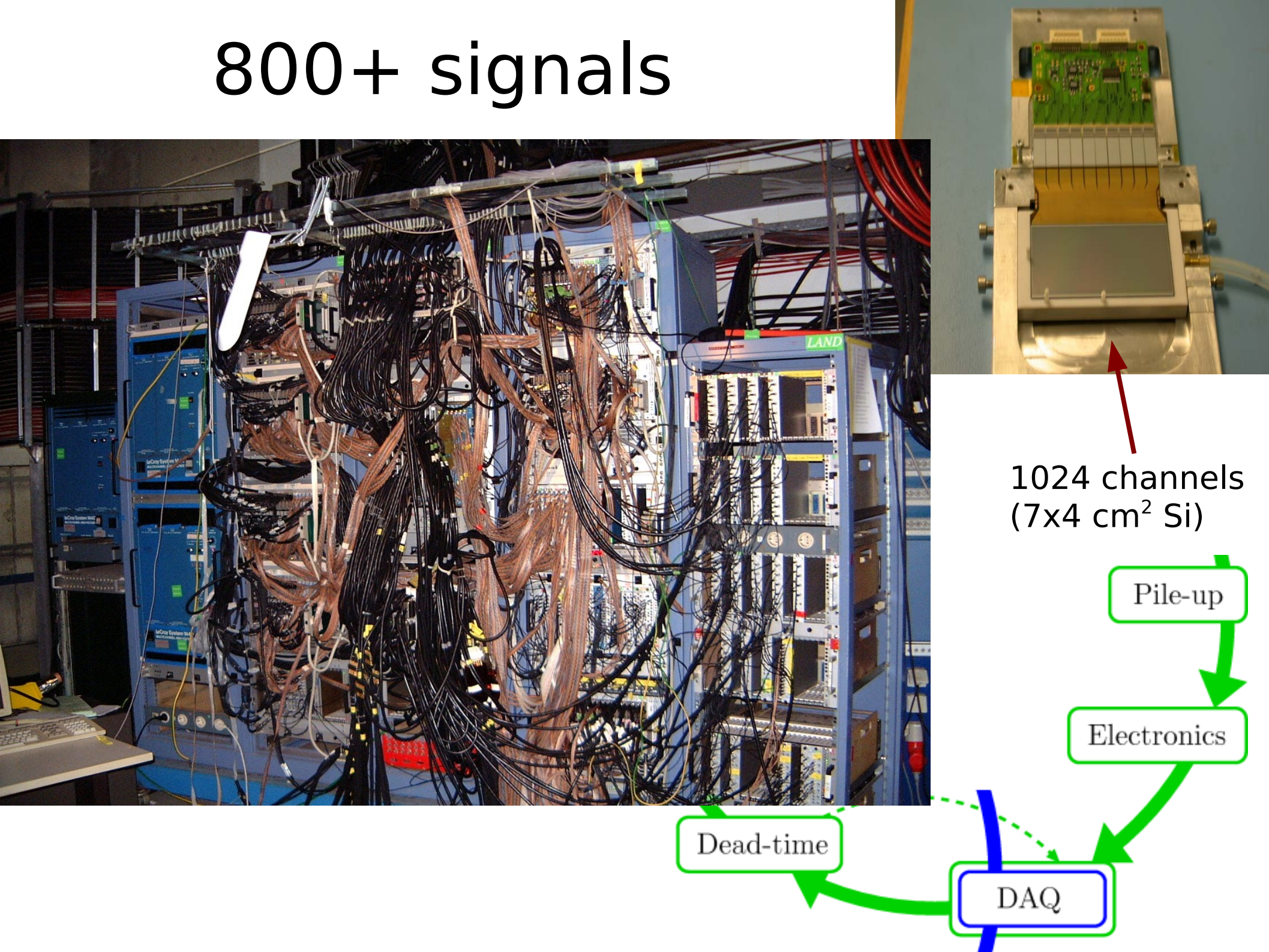
2 PMTs per
paddle



Time + amplitude \rightarrow 800 signals

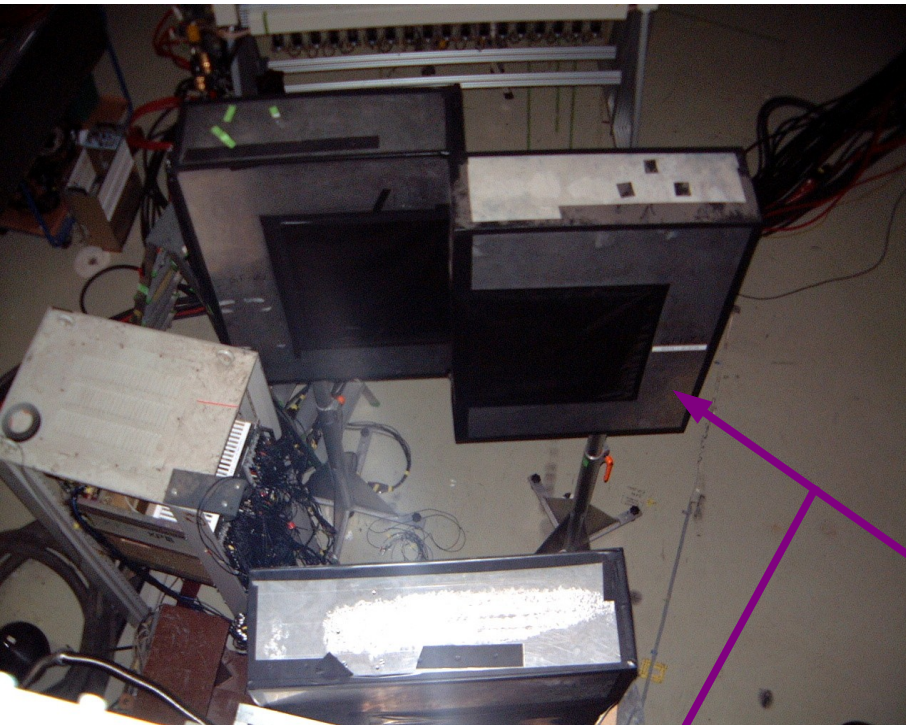


800+ signals



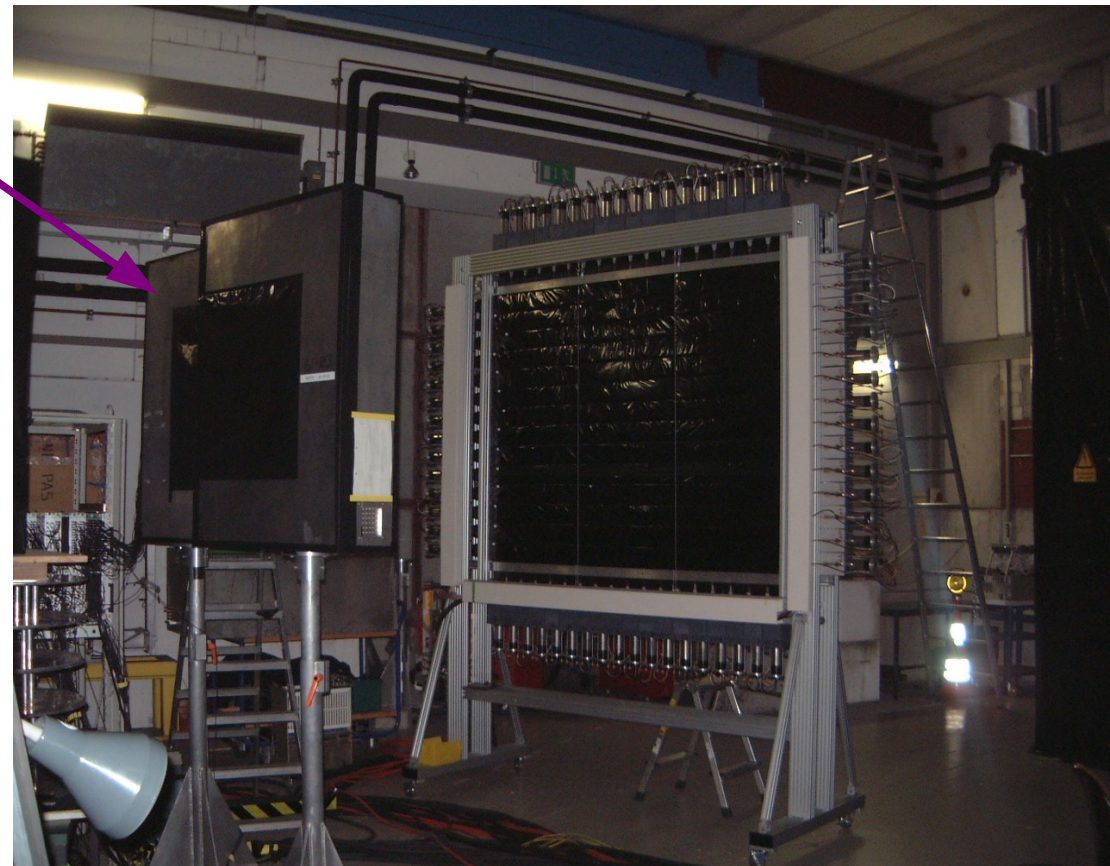
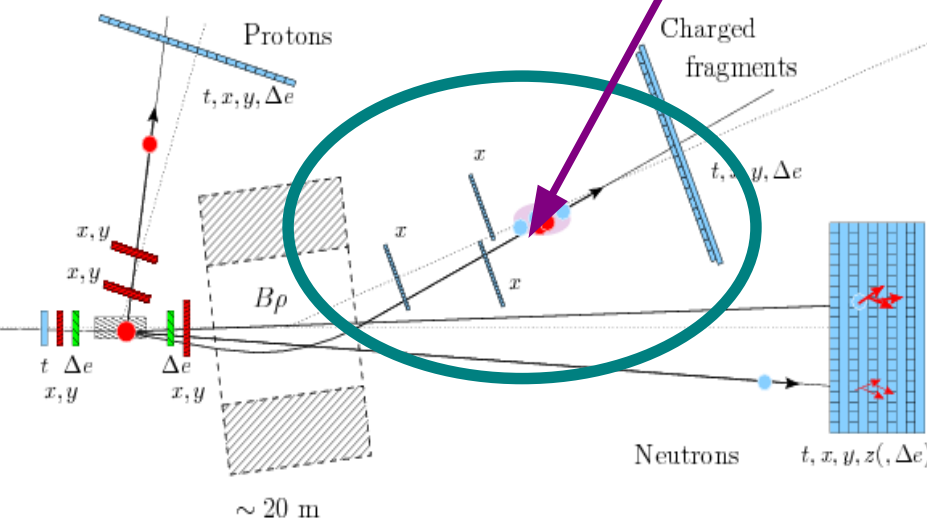
GFI – Großer Fiber Detektor

Large scintillating fibre detectors



500 scintillating fibres per detector

Coupled with lightguides to a position-sensitive photomultiplier (PSPM)



500 scintillating fibres (1.05 mm pitch) → 34(!) read-out channels

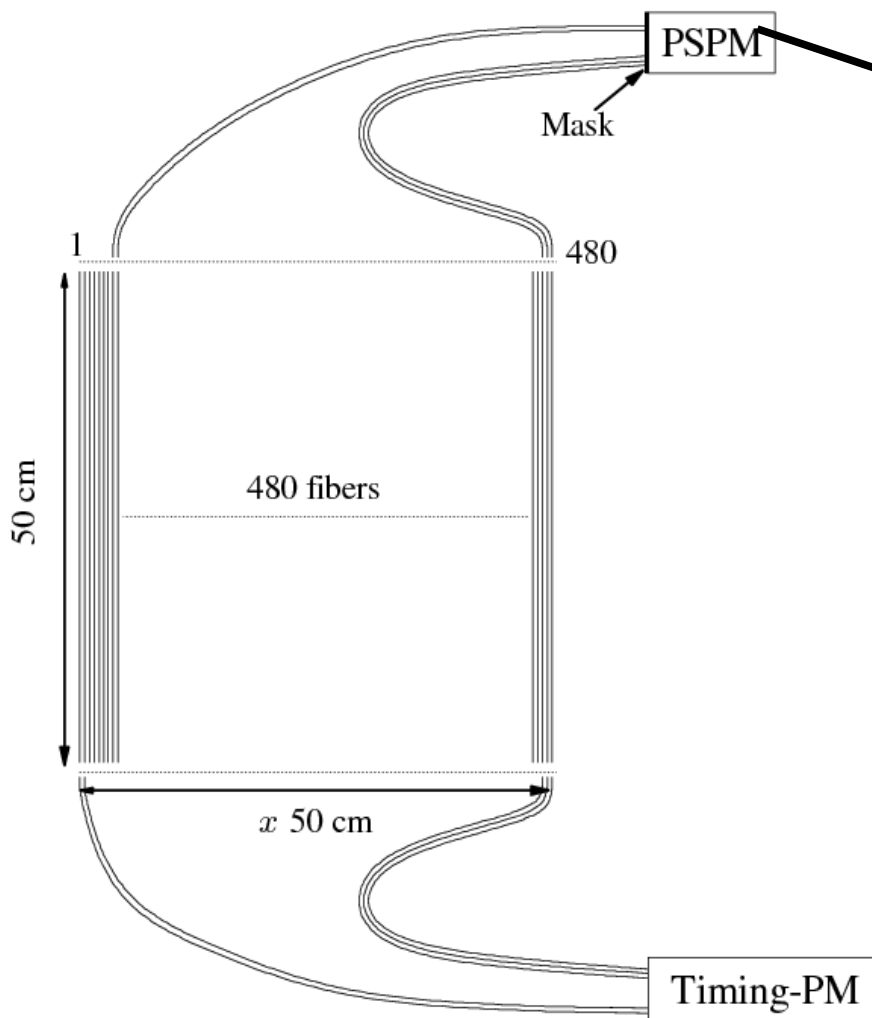


Fig. 1. Schematic view of a scintillating fibre detector.

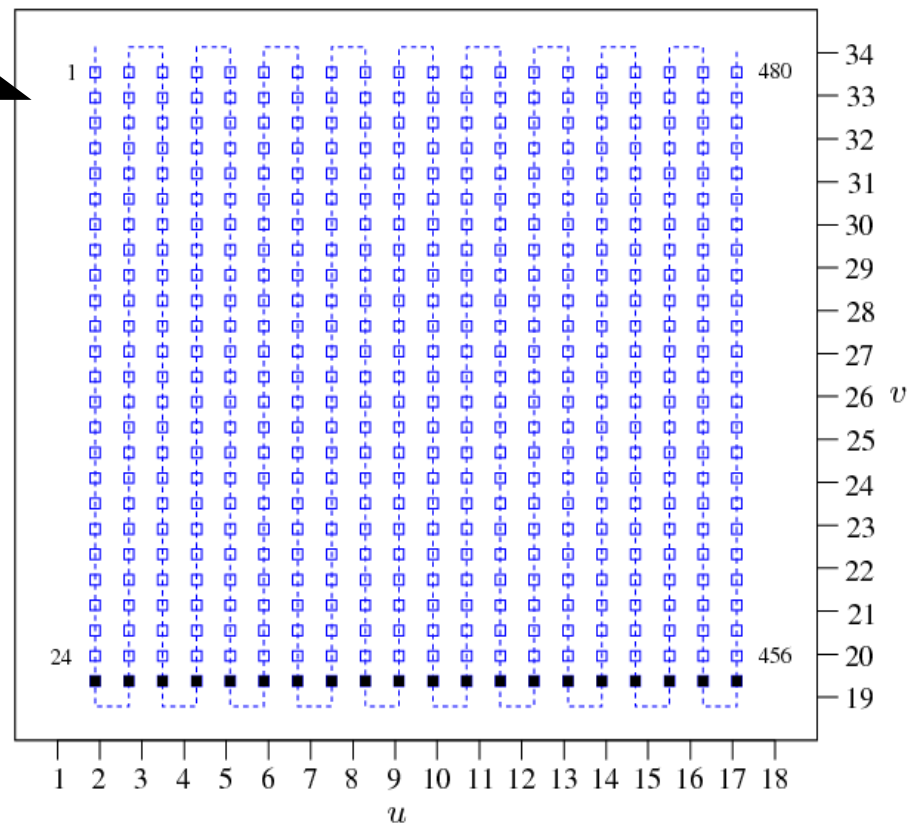


Fig. 2. Mask for fixing one end of the scintillating fibres to the position-sensitive photomultiplier (PSPM). Dark squares indicate unused holes. The dotted line indicates the meander-like ordering of the fibres. The relative position of the anode wires of the PSPM are indicated as well.

Determining the hit fibre

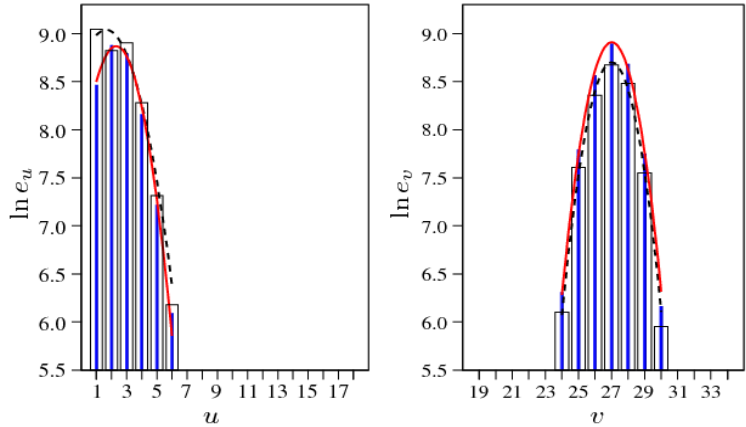
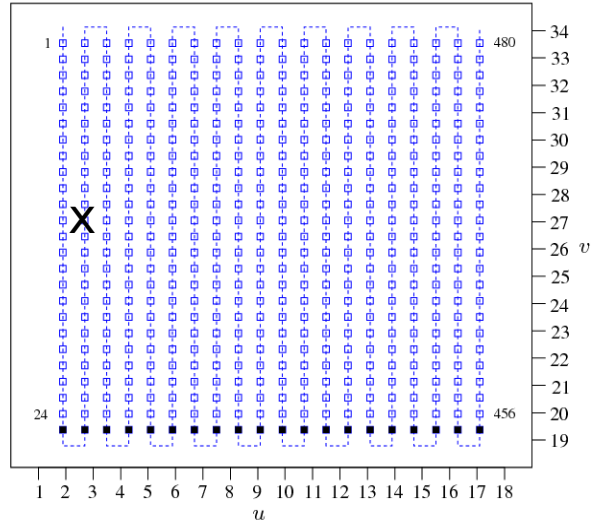
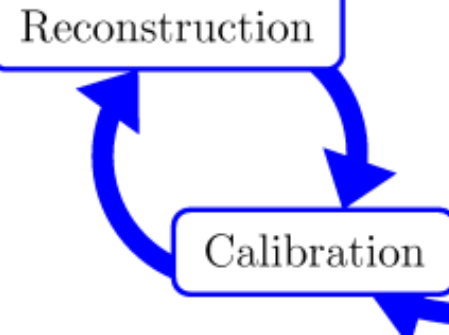


Fig. 3. Typical distributions of charge in the anode wires. The open and the filled (blue) vertical bars represent the natural logarithm of the signal heights recorded in the corresponding wire in a arbitrary unit before and after gain matching, respectively. The dotted and the continuous (red) lines are parabola fits before and after gain matching.

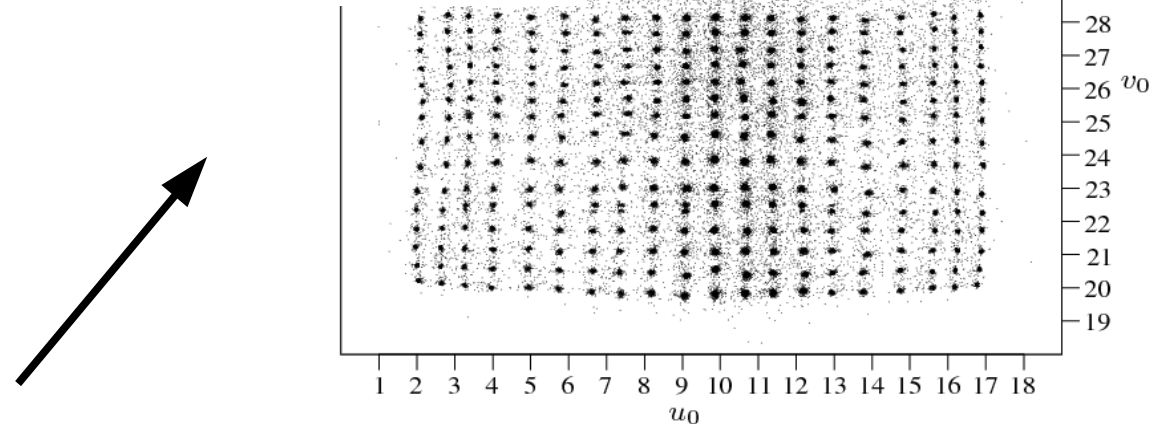
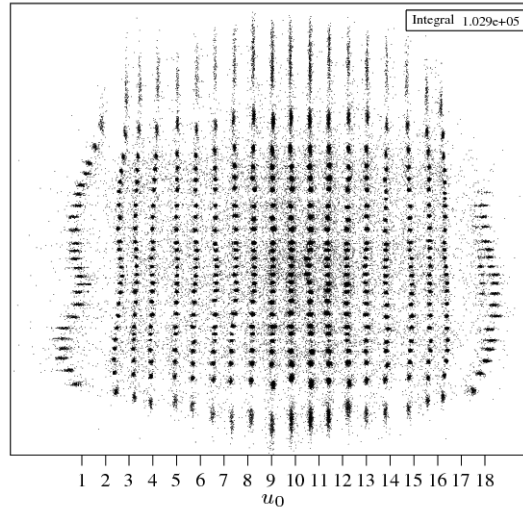


Fig. 4. Reconstructed image of the fibre mask before (top) and after (bottom) gain matching using a ^{58}Ni beam of 650A MeV. Each cluster of dots corresponds to a fibre. The increased number of accepted hits (Integral) in the gain matched panel is discussed in the text.

(PSPM) resolution depends on the deposited energy (ion Z)

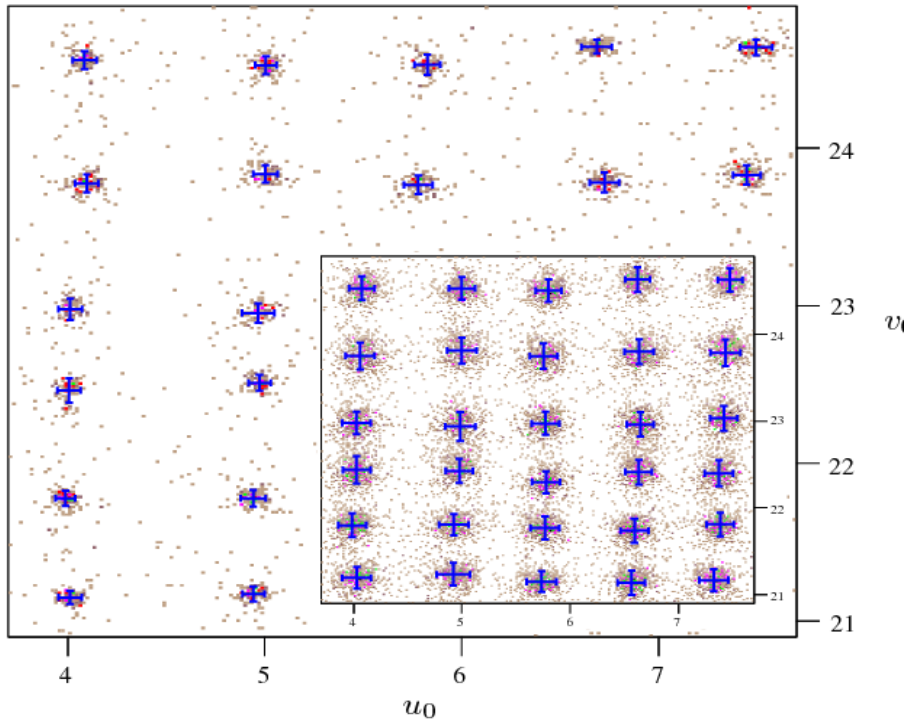


Fig. 5. Part of the 2-dimensional (u_0 , v_0) histogram, with 1000×1000 bins, used to find the mean position and width of the clusters for a 650 A MeV ^{58}Ni beam. The mean positions of the clusters are indicated by crosses. The extents of the crosses correspond to the widths (FWHM) of the clusters. Inset shows the same plot for a 400 A MeV ^{12}C beam.

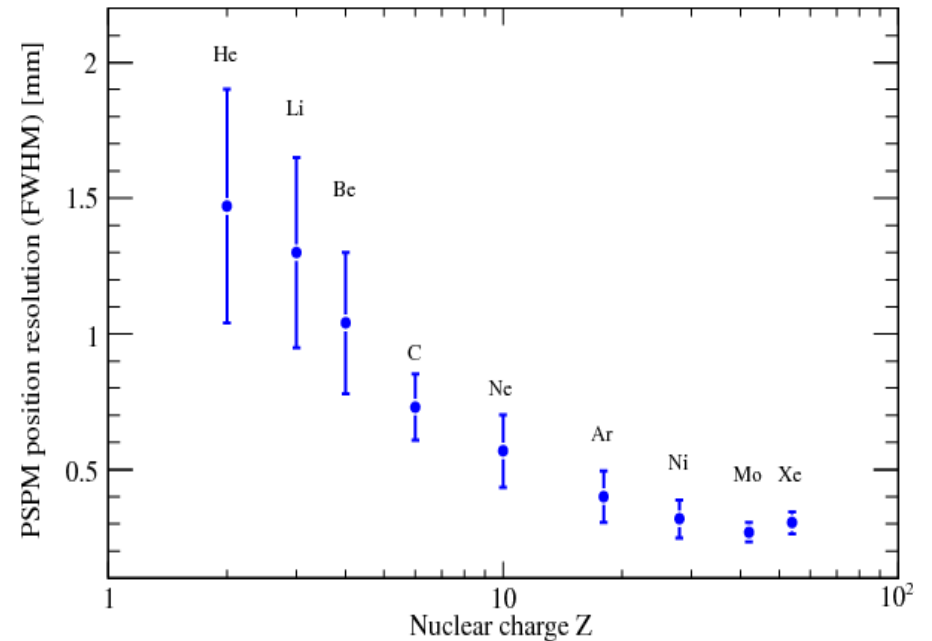
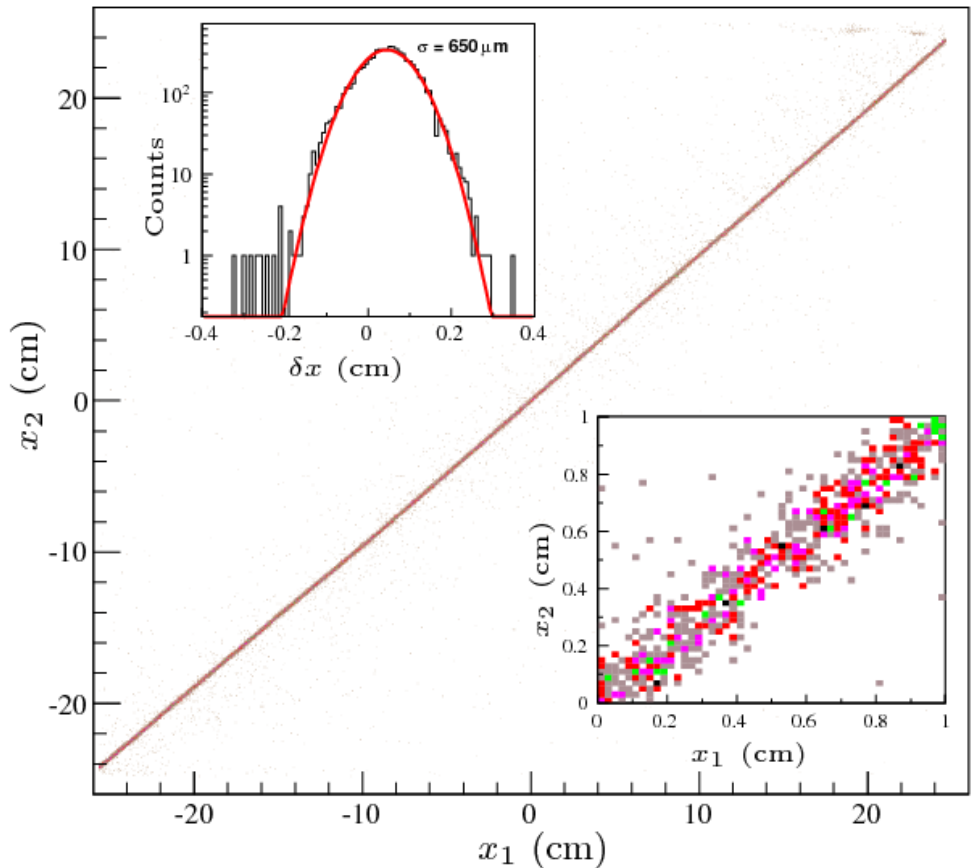


Fig. 6. Position resolution of a PSPM for projectiles of different charges corresponding to different amounts of light produced in the scintillating fibres. The error bars indicate the variation of the resolution over the area of the photocathode. The distance between two fibres is 3.0 mm in u and 2.2 mm in v .

Resolution (S287, Ni ions)



$$x_{\text{GFI1}} - x_{\text{GFI2}}$$

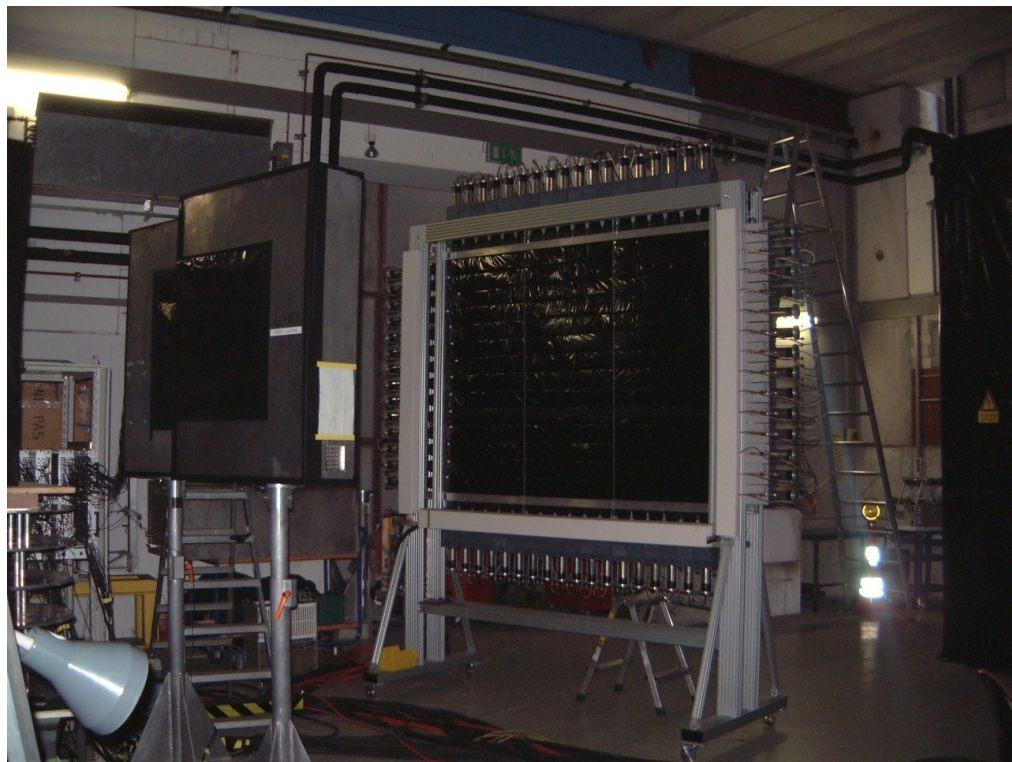
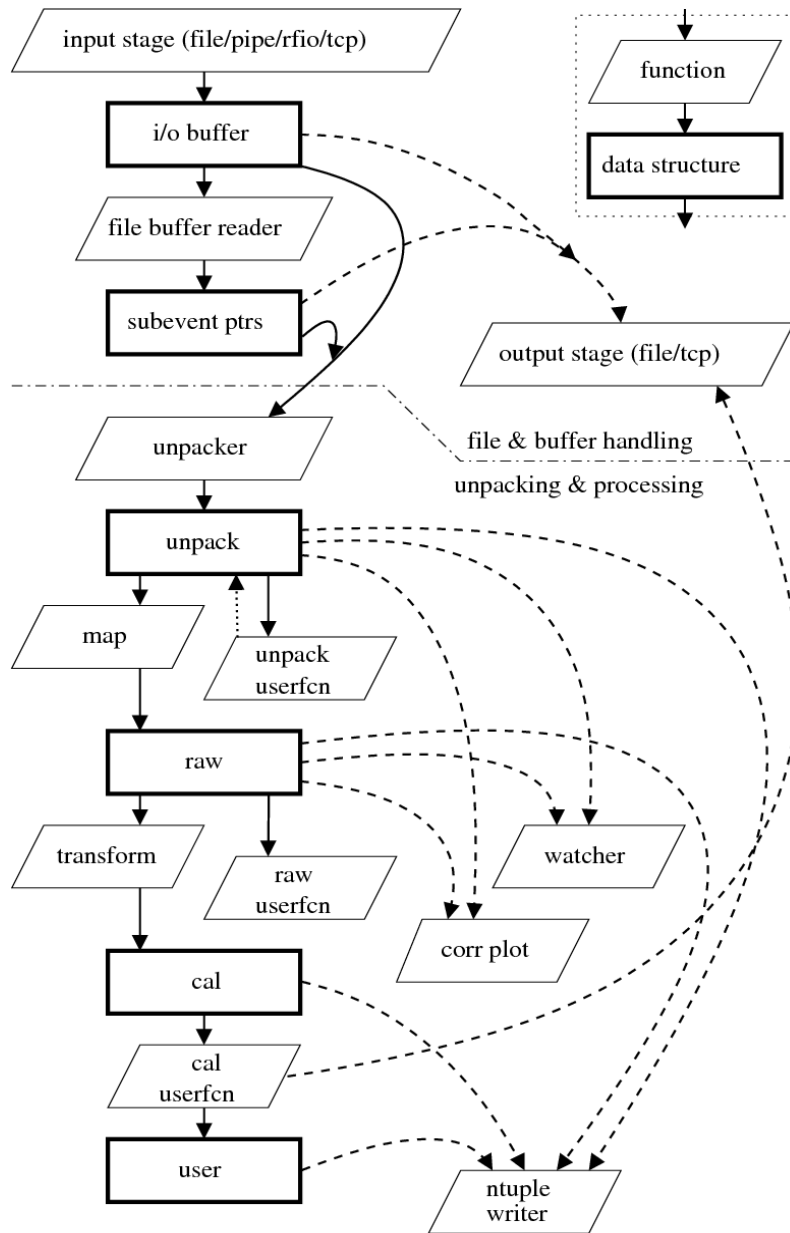


Fig. 8. The reconstructed position correlation between two fibre detectors, ~ 40 cm apart, for a 650 A MeV ^{58}Ni beam. Inset (bottom) shows a (magnified) part of the same plot corresponding to ~ 10 fibres. Inset (top) shows the difference between the position interpolated from two fibre detectors and the measured position in a third fibre detector along with a Gaussian fit.

UCESB – unpack & check every single bit



'Quick-n-dirty' generic unpacking
and data 'quality' monitor

Unpack code generation from C
structure-like specification:

```
SUPER_TDC(slot)
{
    UINT32 value;
}
SUBEVENT(ONE_CRATE)
{
    tdc1 = SUPER_TDC(slot=5);
    tdc2 = SUPER_TDC(slot=6);
}
EVENT
{
    crate1 = ONE_CRATE(type=5);
}
```

Unpacking

Mapping

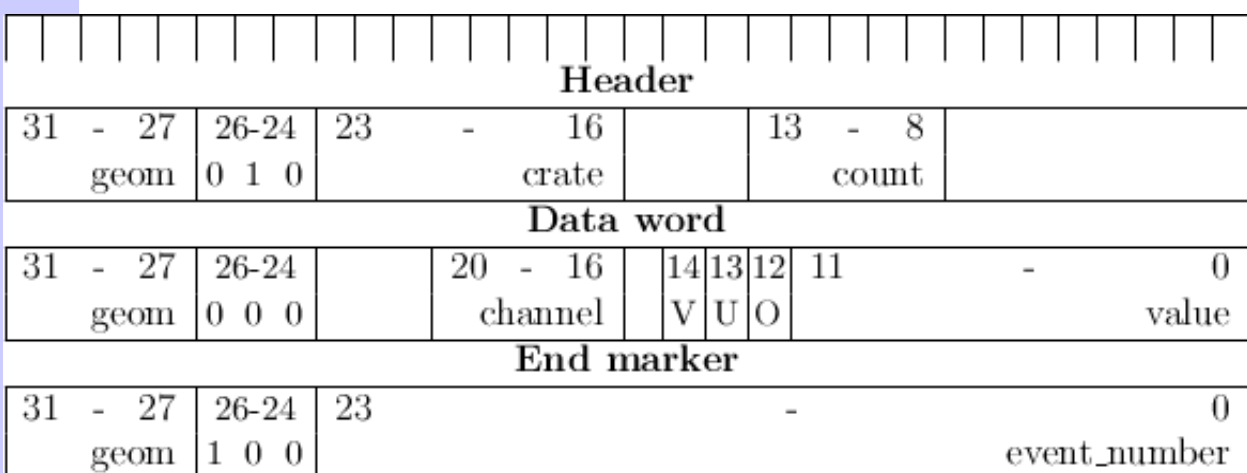
Module .spec structure

```
VME_CAEN_V775(geom,crate)
{
    MEMBER(DATA12_OVERFLOW data[32] ZERO_SUPPRESS);

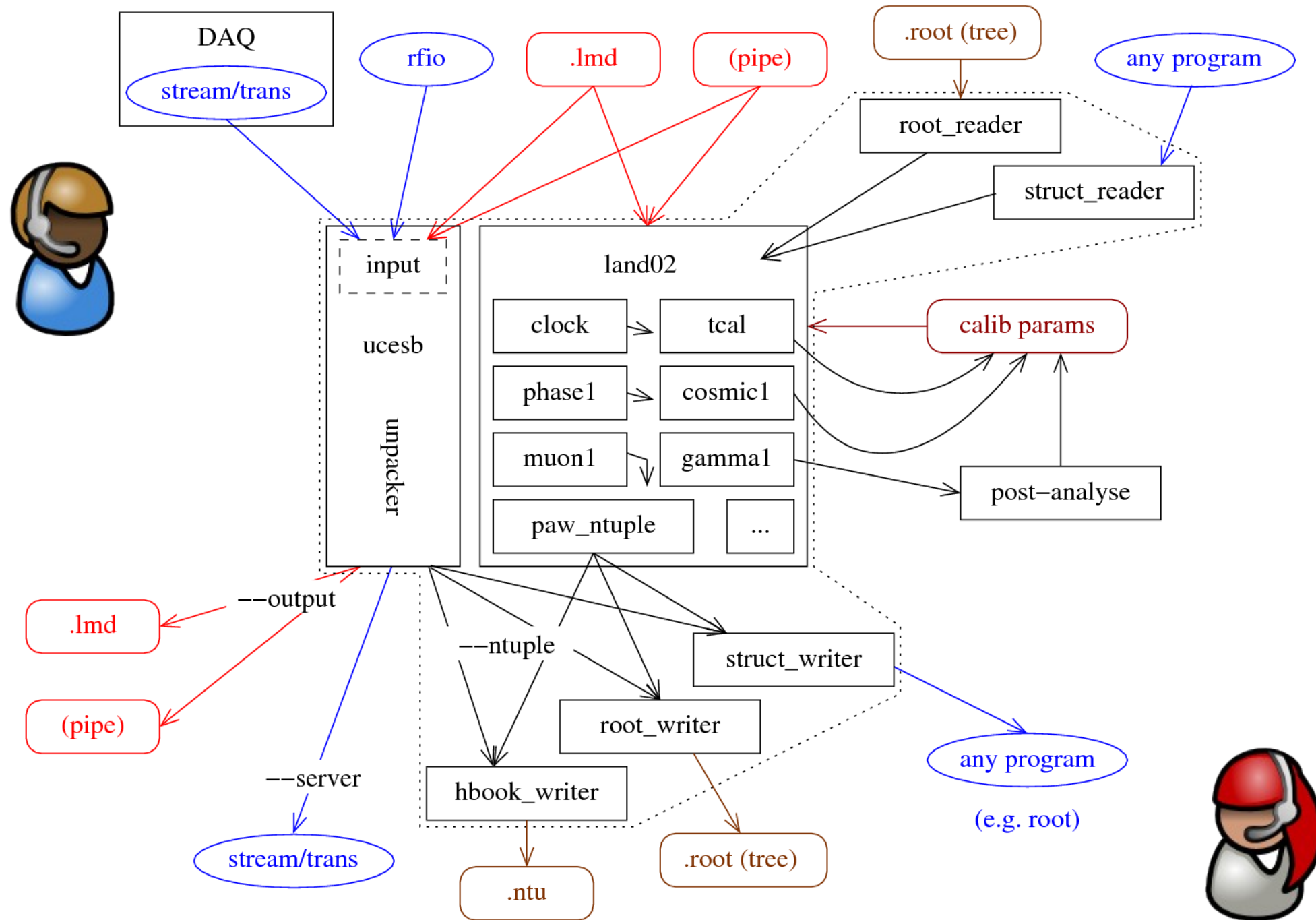
    UINT32 header NOENCODE {
        8_13: count;
        16_23: crate = MATCH(crate);
        24_26: 0b010;
        27_31: geom = MATCH(geom);
    }
    list(0<=index<header.count) {
        UINT32 ch_data NOENCODE {
            0_11: value;
            12: overflow;
            13: underflow;
            14: valid;
            16_20: channel;
            24_26: 0b000;
            27_31: geom = CHECK(geom);

            ENCODE(data[channel],(value=value,overflow=overflow));
        }
    }
    UINT32 eob {
        0_23: event_number;
        24_26: 0b100;
        27_31: geom = CHECK(geom);
    }
}
```

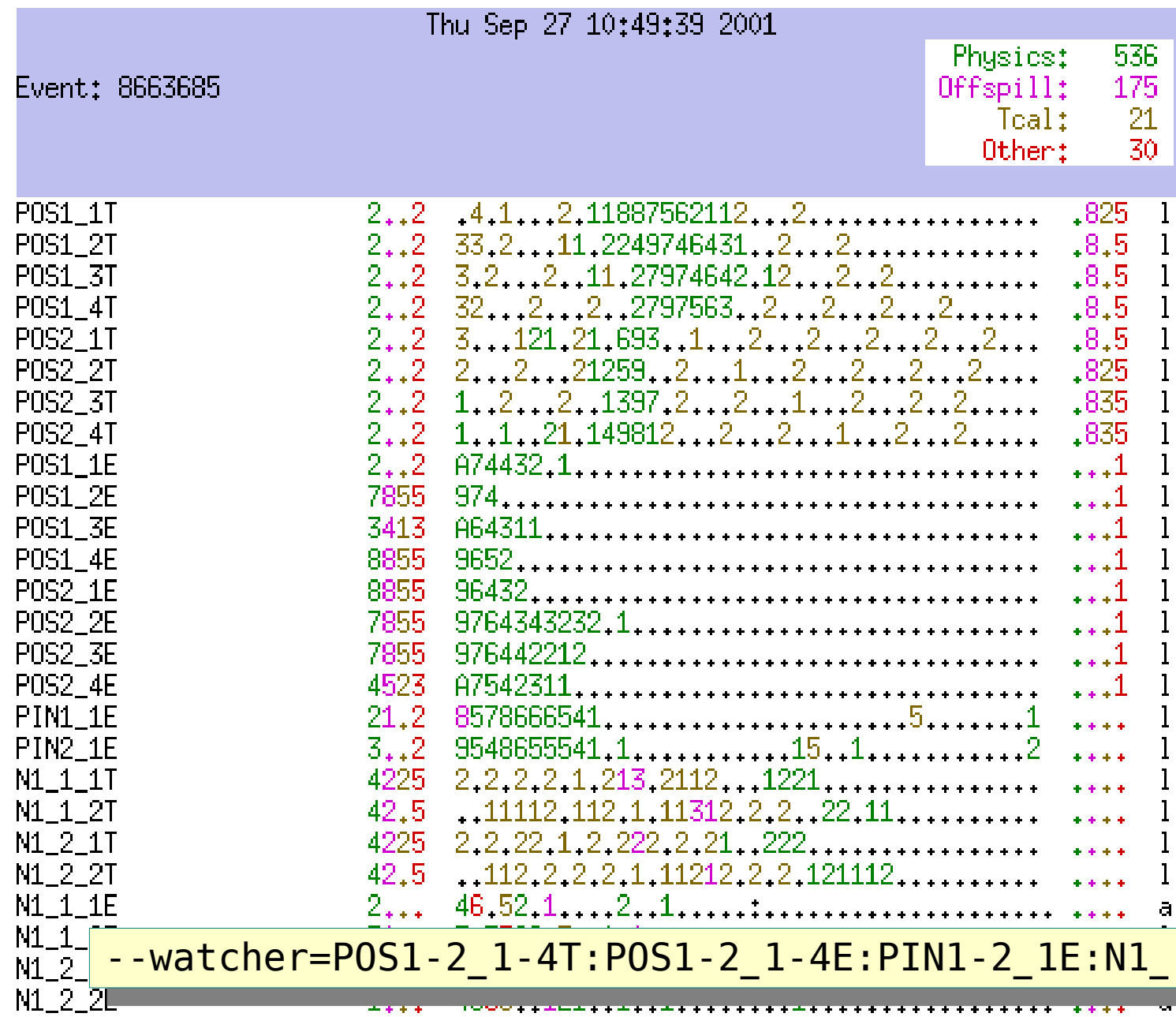
CAEN V775 (TDC) data format:



ucesb/(land02) interaction



Watcher – the DAQscope



Each line is a histogram for one raw channel

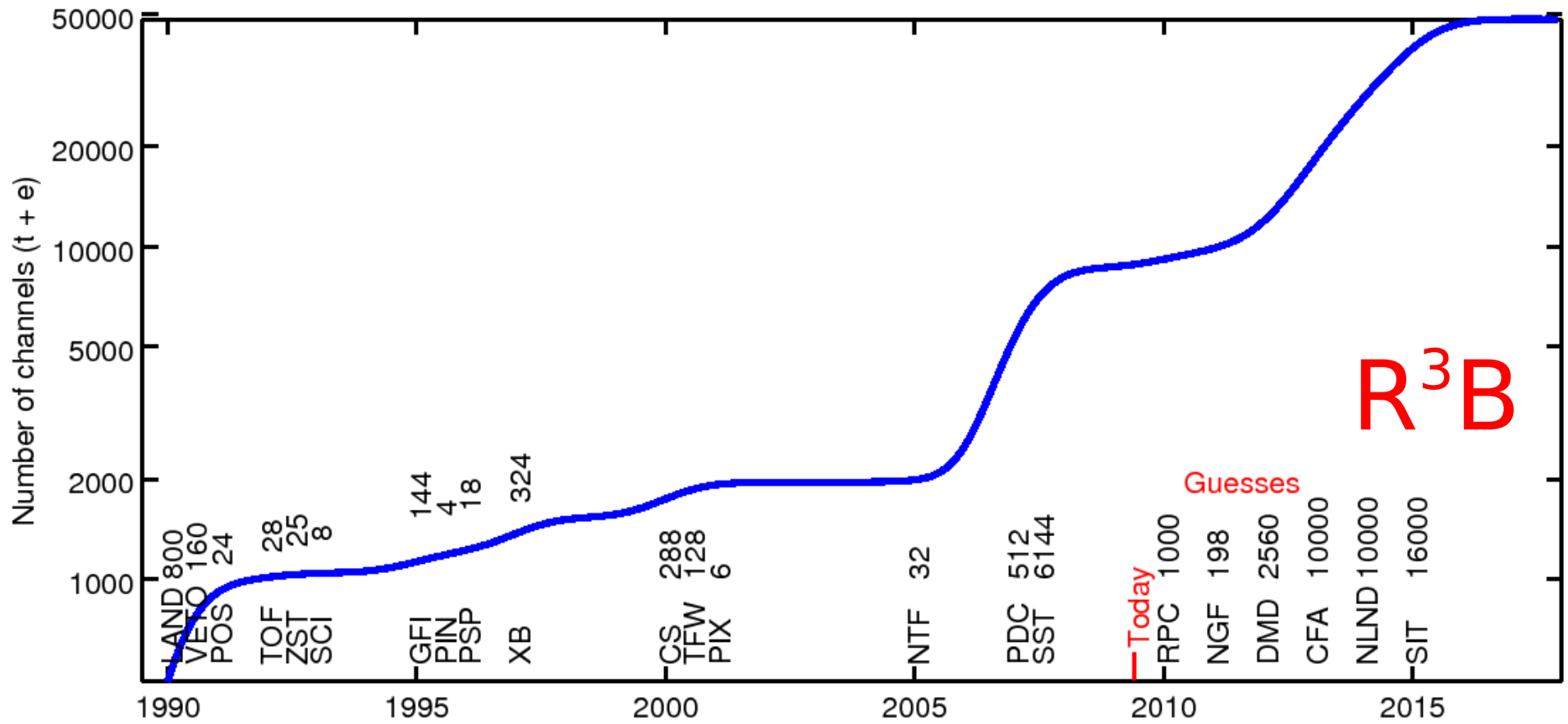
Values are log₂ of bin content

Stored zeros and overflow

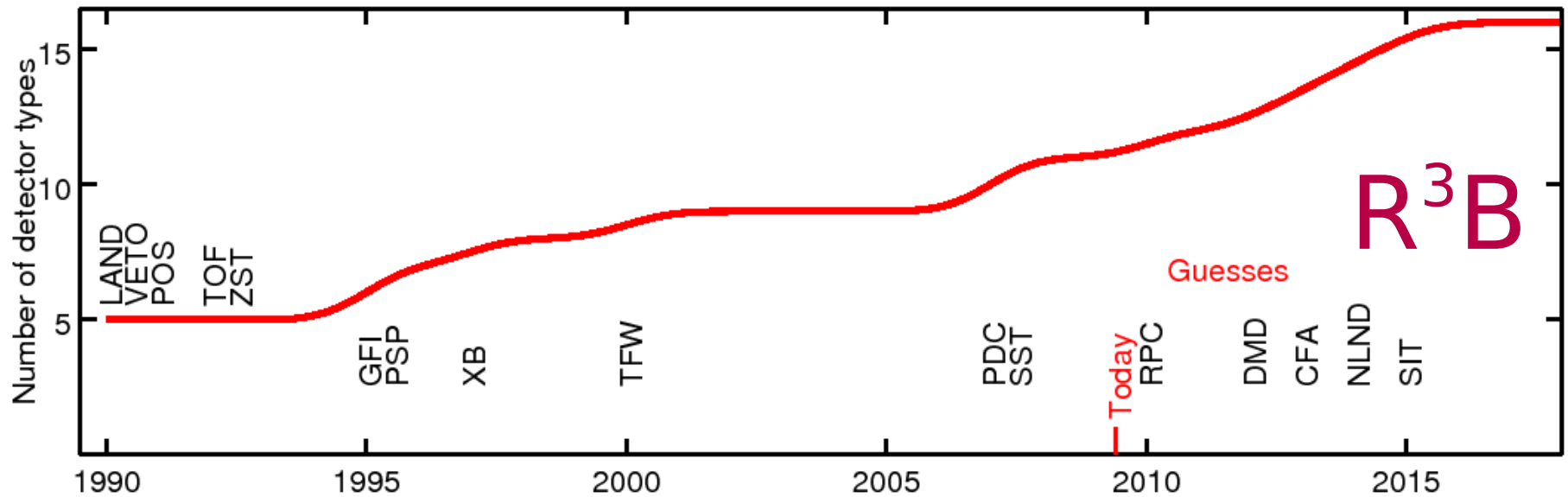
Colour by most contributing trigger type

Spill synchronized

ALADiN-LAND History I – channel counts



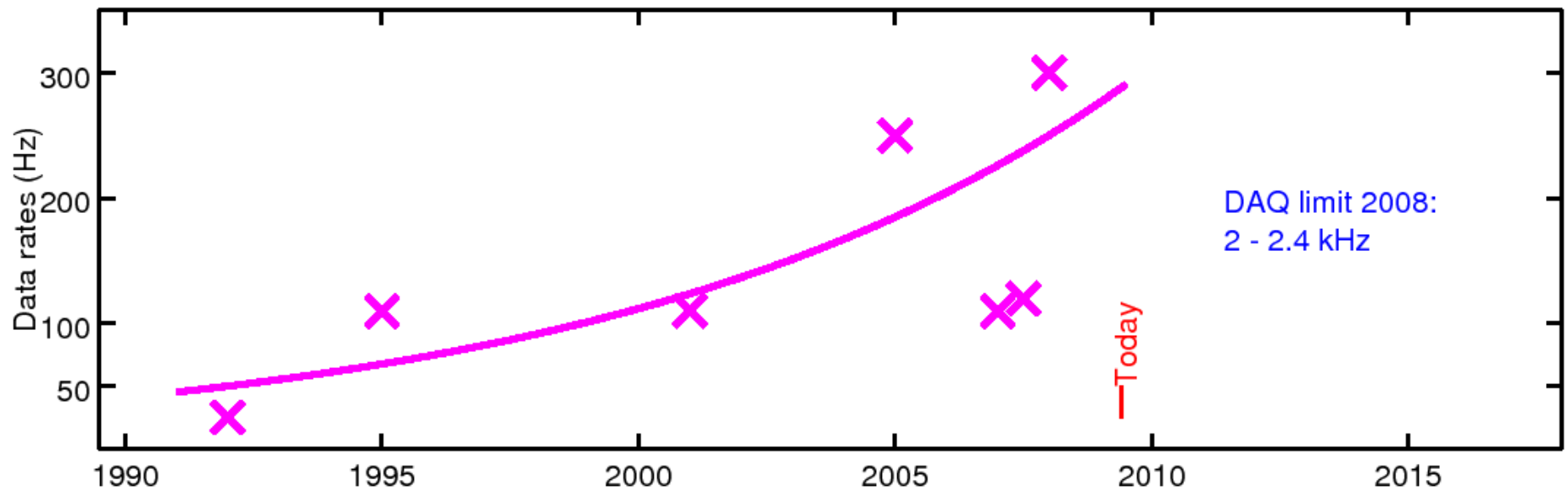
ALADiN-LAND History II – detector types



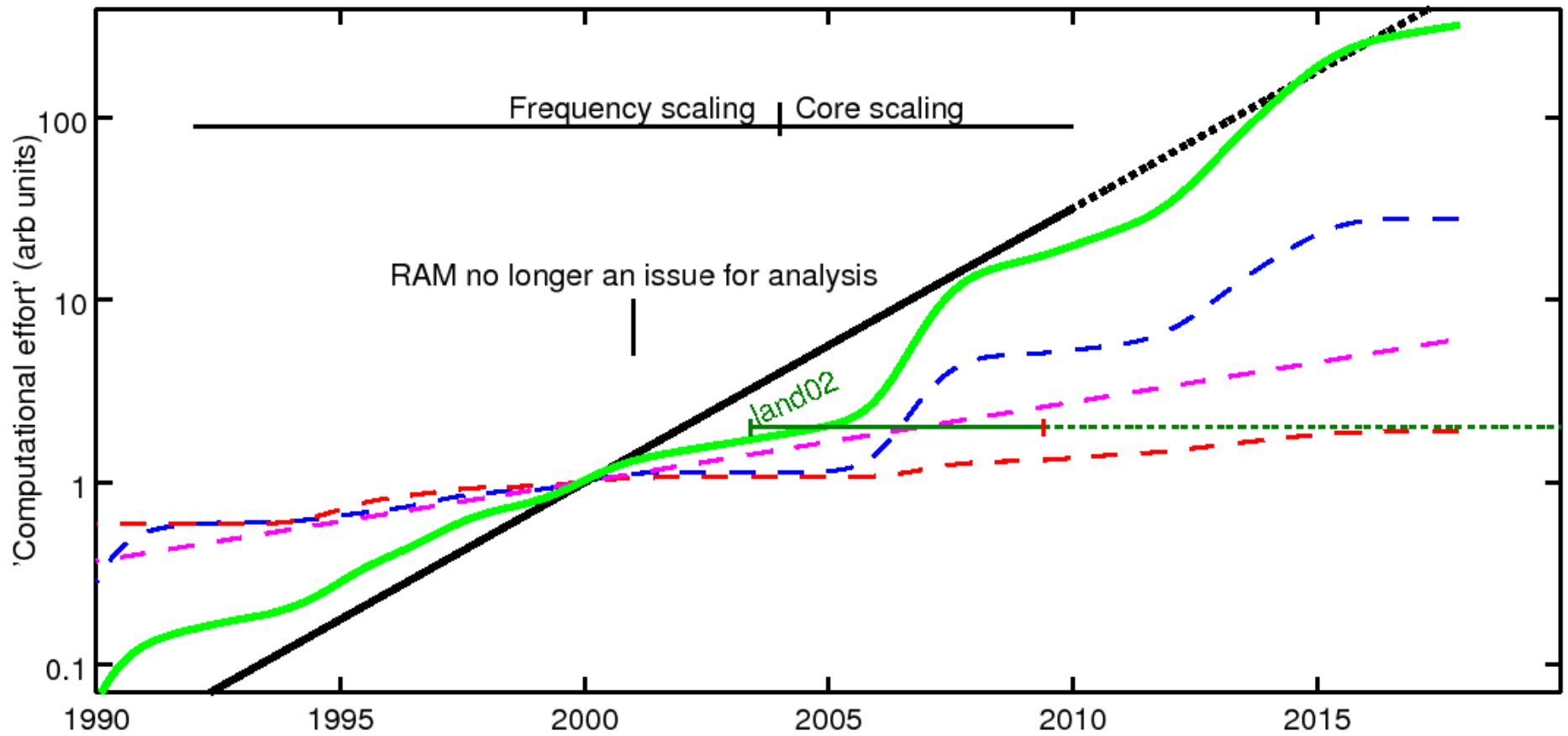
Each detector *type* requires routines for

- Calibration
- Reconstruction

ALADiN-LAND History III – data rates



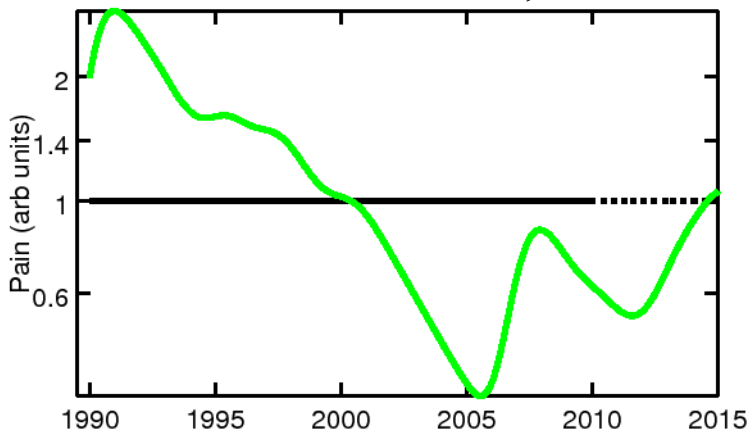
Growing with Moore's law



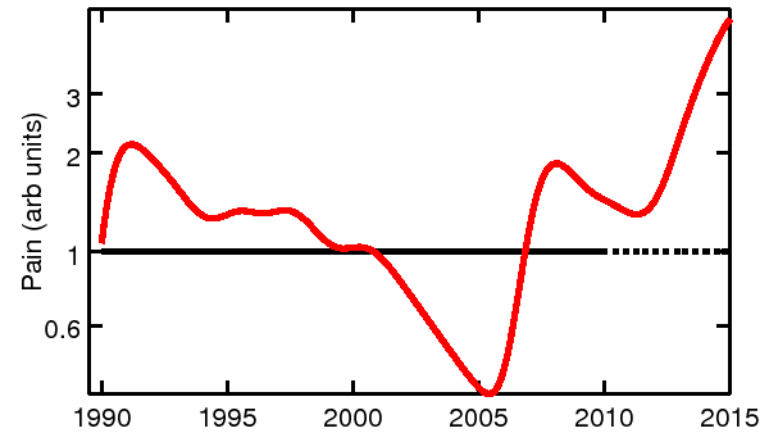
'Easy' scaling valid under assumption of efficient use of computers (i.e. adequate **software**)

Software is an issue

- Capable calibration methods and routines?
- Efficient reconstruction?
- Slow control params?



*sqrt(#ch)



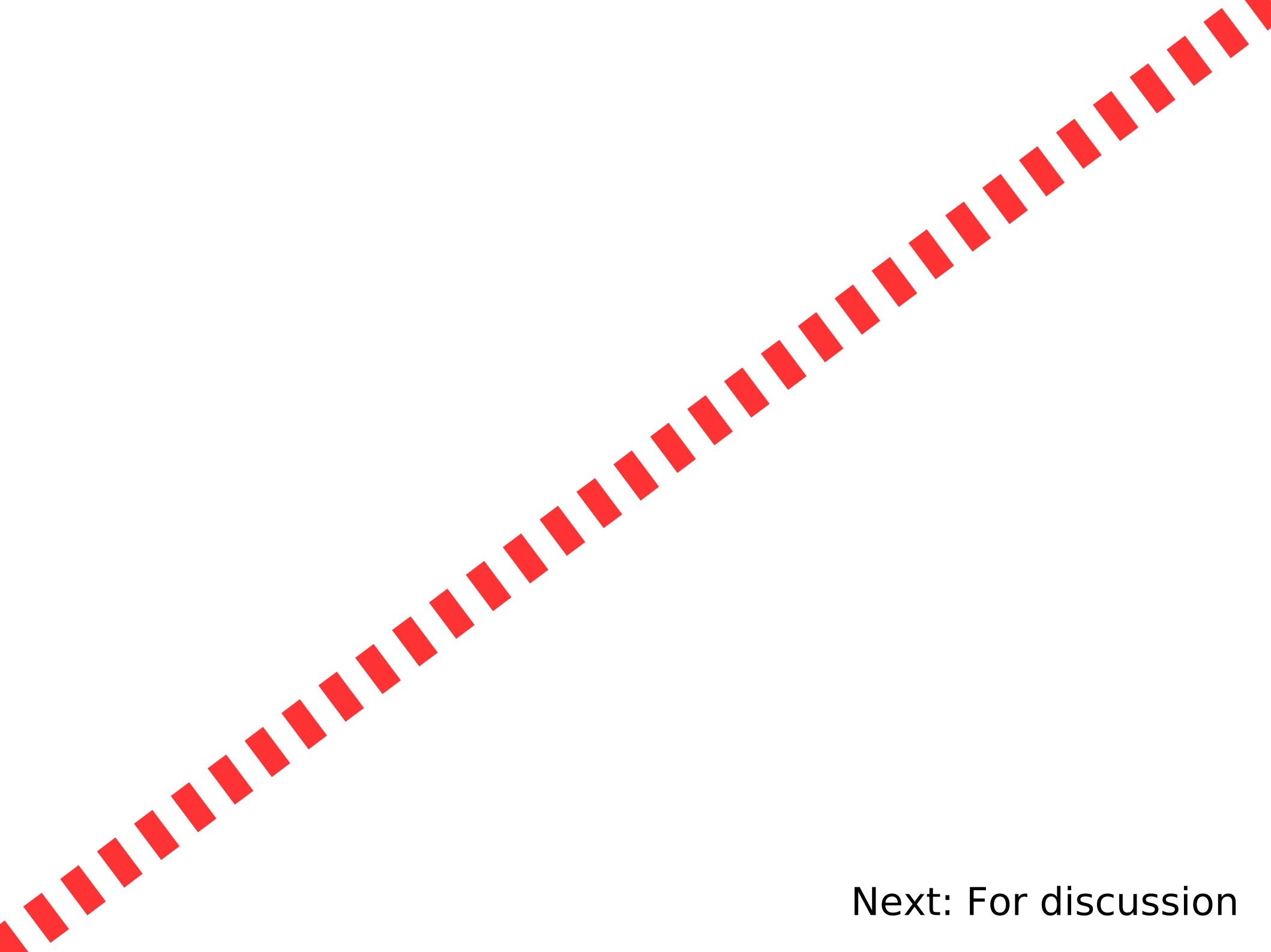
Improvements in computer hardware can handle the increase in data sizes

Unless the software(s) fulfil the requirements of the complex setup, then no amount of computing hardware will help to extract the correct data!

Finale!

Thank you!

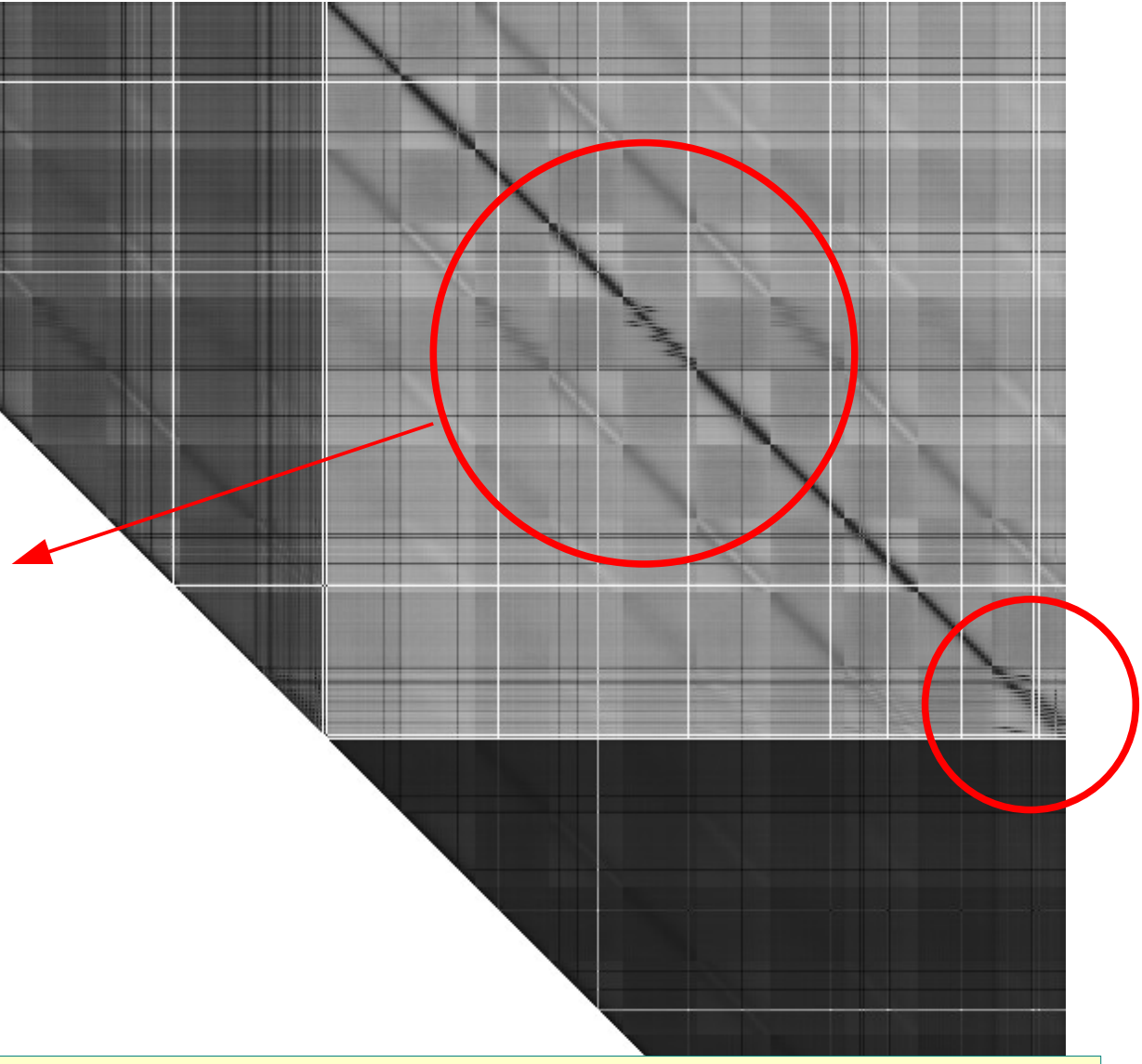
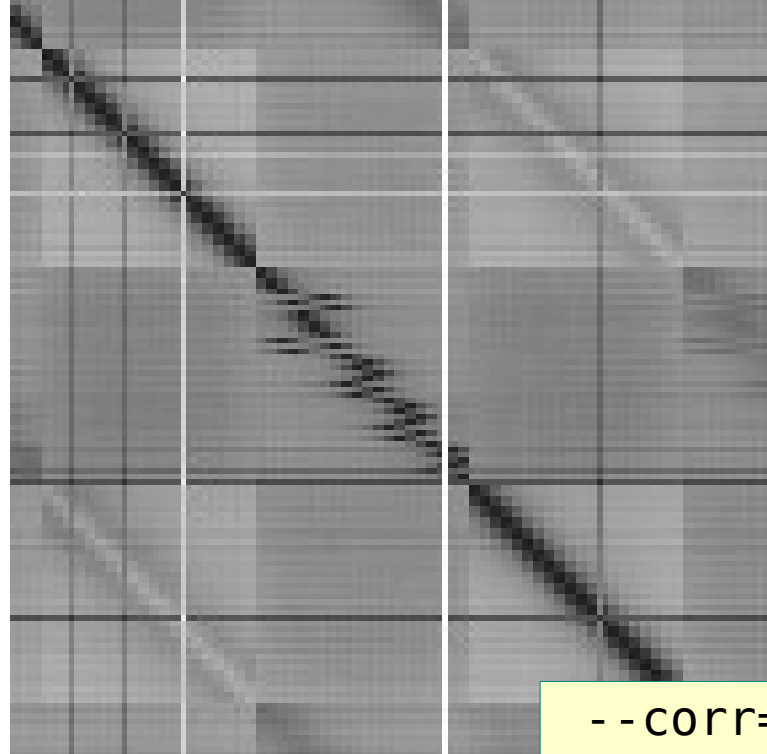
A whole lot of **FUN!**



Next: For discussion

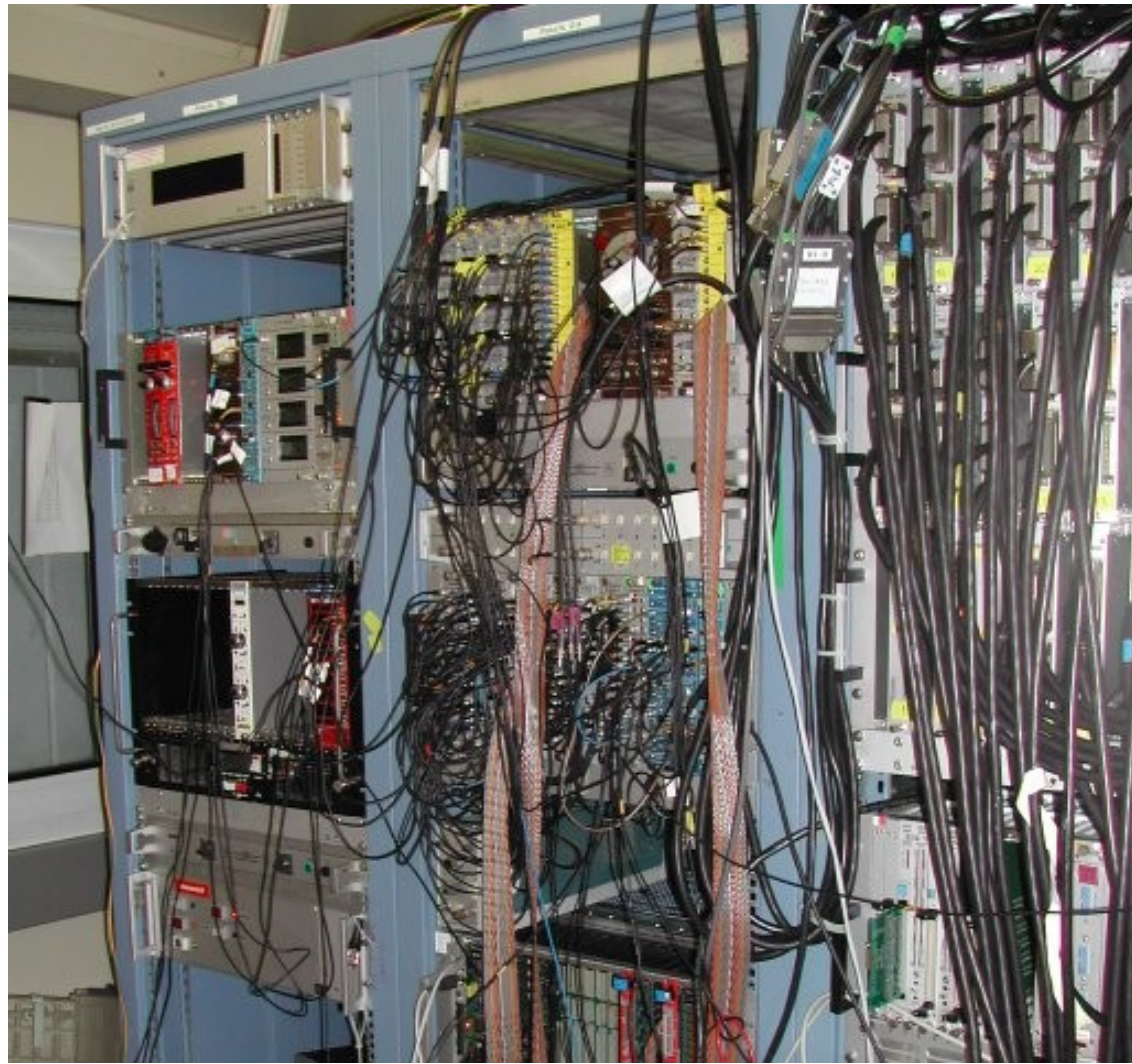
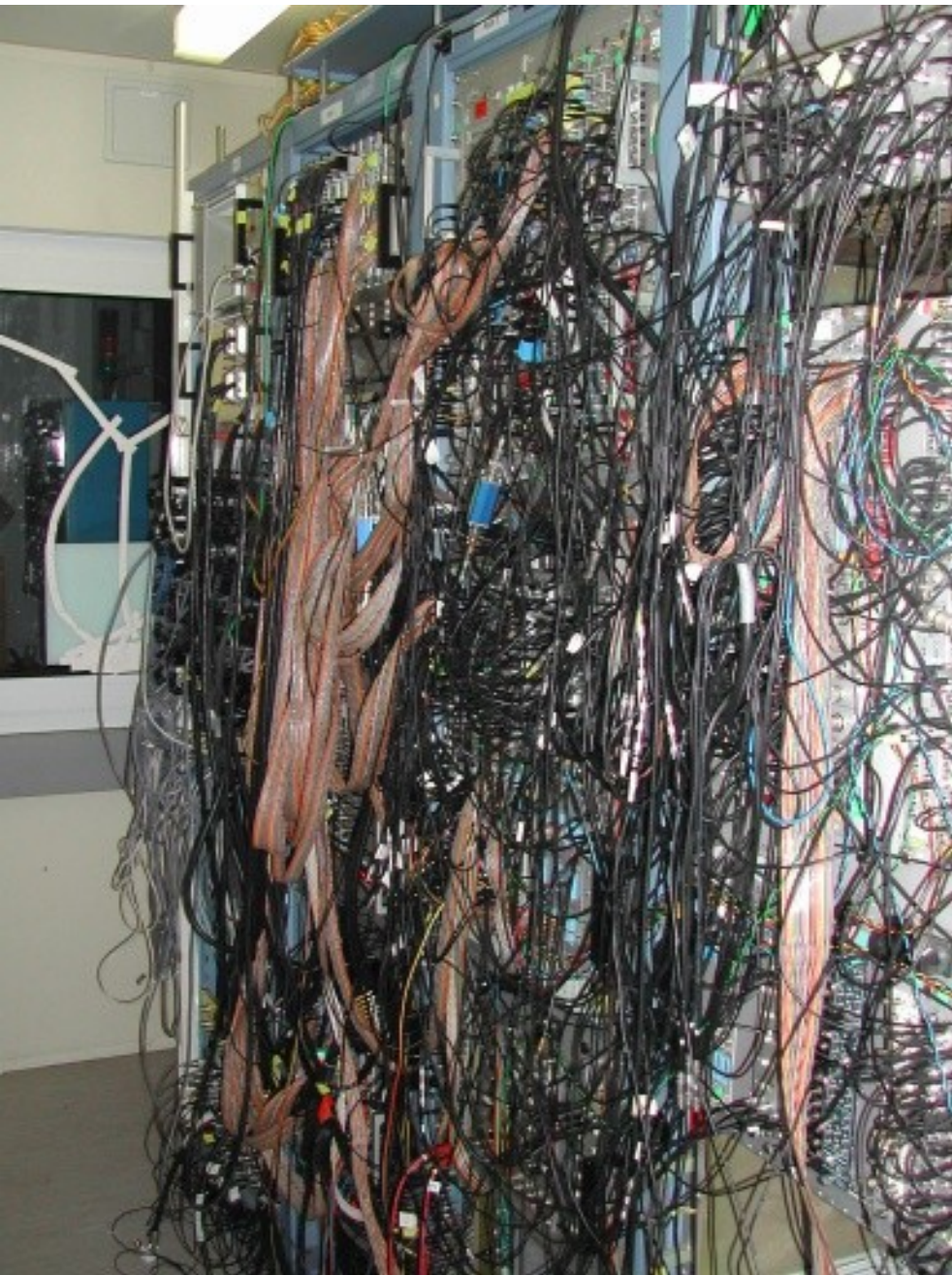
Quickly finding LAND cable mismap

8-fold cable
documentation
problem



--corr=N1-10_1-20_1-2T:N1-10_1-20_1-2T,n_cosm.png

Just a few cables...



Solution / workaround ----->

Support tool: cable documentation

CF8103(r12c2s1)

```
{  
    SERIAL("LCF6343"); // Comments
```

```
in1_8: "N11 CFTN1" <- , r13c1s1(SPLIT)/t1_8;  
th1_8: "1/1"          -> , r11c1s1(SCALER)/in0_7;  
tb1_8: "CR2 SL1"      -> , .s15(DELAY)/in1_8;
```

```
m:           .c11s3/in1;  
test:        .s23/out1;  
mux_tb:      .s22/in1a;  
mux_e:       .s22/in5a;  
mux_mon:    .s22/in9a;
```

```
}
```

C-like text format.

Parsed and checked for consistency.

(Every cable documented twice – at both ends.)

Checker generates tables for unpacking and slow-control.

Documentation

